The role of TXNIP in the hepatic glucose homeostasis

Seong Ho Jo

Department of Medical Science

The Graduate School, Yonsei University

The role of TXNIP in the hepatic glucose homeostasis

Directed by Professor Yong Ho Ahn

The Doctoral Dissertation submitted to
the Department of Medical Science
the Graduate School of Yonsei University
in partial fulfillment of the requirements
for the degree of Doctor of Philosophy

Seong Ho Jo

June 2014

This certifies that the Doctoral Dissertation

of Seong Ho Jo is approved.

Thesis Supervisor: Yong Ho Ahn

Thesis Committee Member#1: Eun Jig Lee

Thesis Committee Member#2: Ho Geun Yoon

Thesis Committee Member#3: Jae Woo Kim

Thesis Committee Member#4: Shin Ae Kang

The Graduate School

Yonsei University

June 2014

ACKNOWLEDGEMENTS

제 인생에서 새로운 시작인 학위 논문을 마무리하게 되었습니다. 실험실 생활을 하며 교수님들과 선후배 및 동료들에게 정말 많은 도움을 받았습니다. 이 논문을 마무리하는데 도움을 주신 모든 분들께 감사인사를 드립니다.

먼저, 부족한 저를 제자로 받아주시고 넓은 아량으로 기다려주시고 지도해주신 저의 멘토 안용호 교수님께 진심으로 감사와 존경의 마음을 전합니다. 앞으로도 교수님의 존함에 누가되지 않게 열정을 가지고 열심히 하겠습니다. 그리고 이 논문을 완성하는데 많은 도움을 주시고 조언을 해주신 이은직 교수님, 김재우 교수님, 윤호근 교수님 그리고 강신애 교수님께 진심으로 감사 드립니다. 또한 생화학 교실에서 많은 조언과 관심을 보내주신 김경섭 교수님, 김건홍 교수님, 허만욱 교수님, 박상욱 교수님 그리고 전경희 교수님께 감사 드립니다.

또한 학위과정 중 많은 도움을 주고 격려를 보내준 가장 중요한 생화학분자생물학 선후배 및 동료들에게 고마움을 전합니다. 이 논문이 나오는데 가장 많은 도움을 주신 우리 팀, 김미영 선생님, 김태현 선생님 그리고 주만에게 고마움을 전합니다. 그리고 제게 큰 도움을 주신 김하일 선생님, 차지영 선생님, 임승순 선생님 그리고 윤미진 선생님께 감사 드립니다. 또한 교실에서 생활하면서 정신적으로 많은 도움을 준 친구 수연, 희은 그리고 김효정 선생님께 진심으로 고마움을 전하고 싶고 고은진 선생님, 양경미 선생님, 효경누나, 재성, 승현, 혜정, 은정, 혜리, 미선,

부남이형, 민경, 동인, 재현, 민영, 해민, 최경화 선생님, 수빈, 한슬, 찬주, 동국, 현숙, 나래, 현진, 유정환 선생님, 윤정, 석준, 승원, 윤희, 정환, 현우, 혁구, 선혁, 혜영, 예슬, 이세정 선생님, 전은지 선생님 그리고 권석철 선생님께 고마움을 전하며 현재 생화학 교실은 아니지만 제게 많은 도움을 준 배진식 선생님, 정윤이형, 유정누나, 혜련, 아름, 미희, 은주, 혜인, 은정, 선영, 혜지, 아라, 그리고 정윤승 선생님께 고마움을 전합니다. 또한 저의 든든한 친구들인 부준, 병익, 영준, 헌 그리고 은영에게 고마움을 전합니다.

제가 힘들 때 중간에 포기하지 않고 의과학을 계속 할 수 있게 많은 도움을 주시고 배려해주신 저의 또 다른 멘토 배외식 교수님께 감사 드리며 같은 분야에서 계속적인 연구를 할 수 있게 정말 큰 도움을 준 대학후배 하영이와 선영이에게 고마움을 전합니다.

마지막으로 제가 학위과정을 마치고 논문을 마무리하는데 가장 큰 힘이 되고 든든한 지원군이 된 우리 가족에게 진심으로 고마움을 전합니다. 저를 믿어준 가족이 있었기에 제가 학위를 마무리 할 수 있었던 것 같습니다. 항상 저를 믿어주시고 지원해주신 부모님, 공부하는 동생을 위해 많은 이해를 해준 누나와 매형에게 감사의 마음을 전하고 저를 배려해주신 장인어른과 장모님, 그리고 처형에게 감사의 마음을 전합니다. 제게 가장 큰 힘과 지원을 해준 나의 아내 영지에게 너무 고맙고 많이 놀아주지도 못한 사랑하는 딸 은아에게 고마움과 사랑을 전합니다.

2014년 6월, 논문을 마무리하며 모든 분께 감사의 마음을 전합니다.

감사합니다.

조 성 호

TABLE OF CONTENTS

LIST OF FIGURES

LIST OF TABLES

Abstract

The role of TXNIP in the hepatic glucose homeostasis

Seong Ho Jo

Department of Medical Science

The Graduate School, Yonsei University

(Directed by Professor Yong Ho Ahn)

Thioredoxin interacting protein (TXNIP) has multiple functions in several pathways involved in the reactive oxygen species (ROS) generation, apoptosis, inflammation and glucose metabolism. TXNIP is upregulated in the hyperglycemic state and represses glucose uptake into several peripheral tissues,

resulting in a homeostatic imbalance of glucose. Although TXNIP has relevance to metabolic syndromes such as obesity and type I and II diabetes mellitus, the role and regulation of TXNIP in liver is unclear. To investigate a metabolic role of TXNIP in the liver, Ad-*Txnip* is administrated to normal mice and an intraperitoneal glucose tolerance test (IPGTT), insulin tolerance test (ITT), and pyruvate tolerance test (PTT) were performed. Overexpression of TXNIP resulted in an impaired glucose, insulin, and pyruvate tolerance in normal mice. After Ad-*Txnip* administration, the expression of genes involved in glucose metabolism, including glucose-6-phosphatase (*G6pc*) and glucokinase (*Gck*) were analysed using qPCR and western blot. Ad-*Txnip* transduction upregulated *G6pc* expression and caused a decrease in *Gck* levels in the liver of normal mice and primary hepatocytes. To understand increased *G6pc* expression in the liver as a result of TXNIP overexpression, pull down assays for TXNIP and small heterodimer partner (SHP) were performed and confirmed that TXNIP

increased *G6pc* expression by forming a complex with SHP which is known to be a negative modulator of gluconeogenesis. To study for the regulation of *Txnip* gene expression, luciferase reporter assays and chromatin immunoprecipitation (ChIP) assays using the *Txnip* promoter were performed to elucidate the interrelationship between carbohydrate response element binding protein (ChREBP) and transcription factor E3 (TFE3) in the regulation of *Txnip* expression. Furthermore, *Txnip* expression in diabetic mouse models was decreased by Ad-*Tfe3* administration, suggesting that TFE3 may play a negative role through competition with ChREBP at the E-box of the *Txnip* promoter. These findings demonstrated that TXNIP impairs glucose and insulin tolerance in mice by upregulating *G6pc* through interaction with SHP and modulating TXNIP expression.

Key words: TXNIP, SHP, ChREBP, TFE3, G6PC, GCK, gluconeogenesis, transcriptional regulation

The role of TXNIP in the hepatic glucose homeostasis

Seong Ho Jo

Department of Medical Science

The Graduate School, Yonsei University

(Directed by Professor Yong Ho Ahn)

I. INTRODUCTION

Obesity-linked inflammation plays a causal role in various metabolic disorders, including type 2 diabetes mellitus, nonalcoholic fatty liver disease, and atherosclerosis. This condition is provoked by ER stress, hypoxia, lipotoxicity, reactive oxygen species, and altered adipokine signaling [1]. Liver plays a key role in maintaining blood glucose level. Hepatic gluconeogenesis is

influenced by varieties of hormones including glucagon, insulin and glucocorticoid, etc. [2]. Other signals affecting hepatic gluconeogenesis include mitochondrial dysfunction [3] and cellular redox states [4]. In the uncontrolled states of diabetes, abnormal production of glucose in the liver contributes to the development of hyperglycemia [5].

Thioredoxin (TRX) is known to be one of the key regulators of cellular metabolism with regard to cellular redox states. TRX mediates a redox signaling by interacting with various transcription factors and signaling proteins [6, 7]. Among those, thioredoxin interacting protein (TXNIP), also called vitamin D upregulated protein (VDUP1) or thioredoxin binding protein (TBP2), is known to be involved in the regulation of various metabolic processes, including fatty acid synthesis and cholesterol accumulation in the liver [8]. TXNIP dissociated from TRX due to reactive oxygen species (ROS) causes an activation of NLRP3 (nucleotide-binding domain and leucine-rich repeat containing protein 3) inflammasome with conversion of pro-IL-1β to active IL-1β [9], which is known to be implicated in the obesity to type 2 diabetes mellitus (T2DM) progression [10]. In vitro, IL-1β over-produced by high glucose, free fatty acid and leptin mediates autoinflammatory response resulting in β-cell death [11]. TXNIP is increased in patients with T2DM [12], however the role of TXNIP in the liver is

largely unknown. Thus, detailed studies on the molecular mechanism governing the control of *Txnip* expression at the transcriptional level and the function of TXNIP in the liver are critical for understanding pathogenesis of T2DM. The expression of *Txnip* is known to be suppressed by insulin [12], *Foxo1* [13] and nitric oxide (NO) [14]. In contrast, glucose [15], glucocorticoid [16], vitamin D [17], Krueppel-like factor 6 (KLF-6) [18] and H_2O_2 [19] upregulate the transcription of *Txnip*. The effect of peroxisome proliferator-activated receptor-gamma (PPARγ) on the expression of *Txnip* gene varies depending on the tissues. In the macrophages, GW929, one of PPARγ agonists increases *Txnip* mRNA level [20], whereas pioglitazone and rosiglitazone, other PPARγ agonists, decreased *Txnip* expression in the kidney derived cell lines [18].

In this study, the *Txnip* expression is increased in STZ-induced mouse model of type I diabetes (STZ-diabetic mice) and *db/db* mice. Overexpression of *Txnip* using adenovirus in normal mice impaired glucose tolerance by upregulating a hepatic glucose-6-phosphatase gene (*G6pc*). Furthermore, transduction of Ad-*Txnip* to the primary cultured hepatocytes increased *G6pc* expression whereas knock-down of *Txnip* using siRNA ameliorated impaired glucose tolerance, suggesting that TXNIP might act at the transcriptional level in the hepatocytes. TXNIP increases the expression of *G6pc* by forming

complex with SHP, a negative modulator of gluconeogenic gene expression. These finding also showed that *Txnip* expression is down-regulated by TFE3, a transcription factor that increases *Irs2* [21] and *Gck* [22] expression. TFE3 down-regulates *Txnip* expression by competing carbohydrate responsive element binding protein (ChREBP) at the carbohydrate responsive element (ChoRE) in the *Txnip* promoter.

II. MATERIALS AND METHODS

1. Cell culture and reagents

HepG2 and HEK293T cells were maintained in Dulbecco's modified Eagle's medium (DMEM) containing 10% (v/v) fetal bovine serum (FBS), 100 units/ml penicillin, and 100 μg/ml streptomycin. Primary hepatocytes were isolated C57BL/6J mouse livers and cultured for 6 h in DMEM high glucose containing 10% (v/v) FBS, 100 units/ml penicillin, 100 μg/ml streptomycin, 10 nmol/l dexamethasone, and 10 nmol/l insulin. And then, FBS, dexamethasone, and insulin were excluded from the medium and cultured for an additional 48 h in the presence or absence of Ad-*Txnip*. Cells were grown at 37°C/5% CO_2 humidified incubator. Glucagon (#G3157) and Insulin (#I9278) were purchased from Sigma-Aldrich (Oakville, Ontario, Canada).

2. Animals

C57BL/6J (C57BL/6JJmsSlc), *db/m*$^{+}$ (C57BLKS/J lar-m^{+}/Lepr^{db}), and *db/db* (C57BLKS/J lar-Lepr^{db}/Lepr^{db}) male mice (Shizuoka laboratory, Hamamatsu, Japan) were fed a regular chow diet and housed under a 12-h light/12-h dark cycle. For the fasted and refed experiments, the mice were divided into fasted or refed groups. The fasted group was fasted for 12 h, and

the refed group was fasted for 12 h and refed a rodent chow diet for 1, 2, 4, 12 or 24 h prior to study. The starting times for experiments were adjusted so that all mice were sacrificed at the same time, which was at the end of dark cycle. STZ-diabetic mice were prepared as described previously [22]. Fourteen days after STZ treatment, mice possessing blood glucose levels greater than 25 mmol/l for 3 consecutive days were used as STZ-diabetic mice. Male *db/db* and *db/m+* mice were used at 10 weeks of age after 2 weeks of acclimation period. All animal experiments were approved by the Institutional Animal Care and Use Committee of Yonsei University College of Medicine.

3. Adenoviral production and Tail Vein Injection

Adenoviral *GFP* (Ad-*GFP*) or *Txnip* (Ad-*Txnip*, a generous gift from R.T. Lee, Harvard Univ.) was injected into the tail vein of control mice at a level of 1×10^9 plaque-forming units (pfu) per mouse. Eight days after adenovirus injection, mice in the fed state were anesthetized with Zoletil (30 mg/kg) and Rompun (10 mg/kg) via intramuscular injection 4 h after an overnight dark cycle. Whole liver was frozen in liquid nitrogen for subsequent mRNA and protein preparation. Adeno-*Tfe3* (Ad-*Tfe3*, a generous gift from N. Yamada, Japan) was injected into the tail vein of control, STZ-diabetic, and *db/db* mice at

1×10^7 (pfu). Basal glucose levels were measured in blood drawn from the mouse tail vein using a glucose monitor (ONE TOUCH Ultra, Life Scan, Milpitas, CA).

4. Glucose tolerance test (GTT), insulin tolerance test (ITT), and pyruvate tolerance test (PTT)

GTT was performed 8 days after adenovirus administration; mice were fasted for 16 h and then glucose was injected intraperitoneally (2 g/kg body weight). Blood glucose levels were monitored at the indicated time points. For the ITT, mice were fasted for 6 h and then insulin (0.75 units/kg Humulin R, Eli Lilly, Indianapolis, IN) was administered intraperitoneally. For the PTT, mice were fasted for 16 h and then injected with sodium pyruvate at a dose of 2 g/kg for lean mice. The area under the curve (AUC) of glucose was calculated during the course of the tests.

5. Metabolites measurement

Blood samples were collected from the inferior vena cava. Plasma insulin levels were measured by enzyme-linked immunosorbent assay (ELISA) kit (ALPCO Immunoassays, Salem, NH). Glycogen content was detected using a

glycogen measurement kit (#ab65620, Abcam, Cambridge, MA).

6. Quantitative real time PCR

Total RNA was isolated from mouse liver or primary hepatocytes using an Easy Spin RNA extraction kit (iNtRON, Gyeonggi-do, Korea), and cDNA was generated using the ImProm-II Reverse Transcription System (Promega, Madison, WI). Quantitative real time PCR (qPCR) was performed using the Step One Real-Time PCR Systems (Applied Biosystems, Foster City, CA). The relative amount of mRNA in each sample was normalized to *Rplp0* transcript levels. The sequences for gene-specific PCR primers are listed in Table 1.

Table 1. Primers used for real-time PCR

Gene symbol	Genbank Accession No.	Sequence (5'-3')
Txnip	NM_023719.2	FW: GTCAGTGTCCCTGGCTCCAAGA RV: AGCTCATCTCAGAGCTCGTCCG
G6pc	NM_008061.3	FW: TGGTAGCCCTGTCTTTCTTTG RV: TTCCAGCATTCACACTTTCCT
Pck1	NM_011044.2	FW: ACACACACACATGCTCACAC RV: ATCACCGCATAGTCTCTGAA
Slc2a2	NM_031197.2	FW: GCAACTGGGTCTGCAATTTT RV: CCAGCGAAGAGGAAGAACAC
Gck	NM_010292.4	FW: CTGTTAGCAGGATGGCAGCTT RV: TTTCCTGGAGAGATGCTGTGG
Irs2	NM_001081212.1	FW: GCCTGGGGATAATGGTGACT RV: TCCATGAGACTTAGCCGCTT
Tfe3	NM_172472.3	FW: CCAGGCTCAGGAACAGGAGA RV: TACTGTTTGACCTGCTGCCG
Srebp1a	NM_023719.2	FW: GGCCGAGATGTGCGAACT RV: TTGTTGATGAGCTGGAGCATGT
Srebp1c	NM_008061.3	FW: GGAGCCATGGATTGCACATT RV: GGCCCGGGAAGTCACTGT
Srebp2	NM_011044.2	FW: CAAGTGGGAGAGTTCCCTGA RV: GCAGGACTTGAAAGCTGGTC

Elovl6	NM_031197.2	FW: GTCGCTGACTCTTGCCGTCTTC RV: TCACCTAGTTCGGGTGCTTTGC
Acacb	NM_010292.4	FW: TATTCCAAGTGGCTTGGGTGGA RV: TCTGGATTCGCCTTCATCTTCG
Fasn	NM_001081212.1	FW: TTTGCTGCCGTGTCCTTCTACC RV: ATGTGCACAGACACCTTCCCGT
Scd1	NM_172472.3	FW: GCCACCTGGCTGGTGAACAG RV: AGCGTACGCACTGGCAGAGTAG
Shp	NM_007475.5	FW: CCAGTATACTTAAGAAGATCCT RV: ACGCATACTCCTTGGGACC
Rplp0	NM_007475.5	FW: GCAGGTGTTTGACAACGGCAG RV: GATGATGGAGTGTGGCACCGA

7. Western blot analysis

Western blot was performed as described previously [22]. Briefly, proteins were transferred to nitrocellulose membrane (Whatman, Germany) and blocked with non-fat milk and incubated with the following primary antibodies: anti-TXNIP (K0205-3, MBL international, Woburn, MA), anti-G6PC (sc-27198), anti-PCK1 (sc-32879), anti-GCK (sc-7908), anti-SHP (sc-30169) and anti-α-Tubulin (sc-5286) (Santa Cruz Biotechnology Inc., Santa Cruz, CA), anti-GLUT2 (AB1342, Millipore, Temecula, CA), anti-TFE3 (ab70008, Abcam, Cambridge, MA), anti-IRS2 (3089) and anti-Myc (2276) (Cell Signaling, St. Louis, MO), anti-Flag (G188, Applied Biological Materials Inc., Richmond, BC), and anti-HA (ADI-MSA-106-E, Enzo Life Sciences, Farmingdale, NY). The protein bands were detected using an Imager (Fujifilm LAS-3000, Fujifilm, Tokyo, Japan).

8. Plasmids

Mouse *Txnip* promoter-luciferase reporter constructs were constructed by amplifying the promoter region of m*Txnip* (-1119/+279) using primers. The PCR products were inserted into the pGL4 basic vector (pGL4b). The serial deletion constructs of the *Txnip* promoter reporter (-879, -600, -400, -200, -138

and -30) were prepared by PCR with *mTxnip* (-1119/+279) as template. Luciferase reporter constructs with the m*G6pc* promoter (-500/+66bp), *mL-Pk* promoter (-697/+106) and *mScd1* (-1175/+300) were prepared by PCR using primers. The PCR products were inserted into the pGL4 basic vector (pGL4b). Expression vectors such as HA-tagged *SHP*, Myc-tagged *Foxo1*, Flag-tagged *ChREBP* (generous gift from Towle HC, Minnesota Univ.), and V5-tagged *Tfe3* were described previously [21]. *Hnf1α*, *Hnf3β* and *Hnf4α* plasmid vectors were generous gift from Im SS (Keimyung Univ). The primers used for amplifying the promoter region are shown in Table 2.

Table 2. Primers used for plasmid constructions

Plasmid		Sequence (5'-3')
***Txnip* -1119**	FW	CTAGGTACCGTGAAACTAACACAGCTCCAGCG
***Txnip* -879**	FW	CTAGGTACCACCTCACAAAGCTGCAGTGAGG
***Txnip* -600**	FW	CTAGGTACCAGCCTTTTATTCTTCAATAGAA
***Txnip* -400**	FW	CTAGGTACCAAATCCTCTCCTAAGCACATTT
***Txnip* -200**	FW	CTAGGTACCGAACAACAACCATTTTCCCCGC
***Txnip* -138**	FW	CTAGGTACCGATTGGTTGGAGGCC TGGTAAAC
***Txnip* -30**	FW	CTAGGTACCGGCTATATAAGCCGTTTCCGGC
***Txnip* +279**	RV	CTACTCGAGGATTGAGCCGAGTGGGTTC
***L-Pk* -697**	FW	CTAGGTACCGTTTCATCTTTGGATTCACAGAGG
***L-Pk* +106**	RV	CTACTCGAGGTCTTTTTGGGACTTAAAGATC
***Scd1* -1175**	FW	CTAGGTACCGGTGTAAAGTTGAGGACTTC
***Scd1* +300**	RV	CTACTCGAGGATGATAGTCAGTTGCTCG

(Restriction enzyme sites are underlined)

9. Transient transfection and luciferase assays

HepG2 cells were plated in 12-well tissue culture dishes at a density of 2×10^5 cells/well in 1 mL DMEM medium. Expression plasmids for *Tfe3* (0, 50, 100, and 200 ng) and *ChREBP* (200 ng), the m*Txnip* promoter reporter (200 ng) and the *Renilla* luciferase plasmid were co-transfected using the FuGENE 6 Transfection Reagent (Roche, Mannheim, Germany) at a ratio of 4:1. For the *G6pc* promoter activity assay, the promoter reporter (200 ng) was used with expression plasmids for *Txnip* (0, 10, 20, 50, 100, and 200 ng), *SHP* (200 ng), *Foxo1* (200 ng), *Hnf1*α (200 ng), *Hnf3*β (200 ng) and *Hnf4*α (200 ng). Total amount of transfected plasmid was adjusted to 600 ng by the addition of empty vector plasmids. For *L-Pk* and *Scd1* promoter assay, HepG2 cells were transfected with *ChREBP* (200 ng), firefly luciferase fusion promoter reporter constructs of *L-Pk* (200 ng) or *Scd1* (200 ng) and expression plasmid Renilla luciferase in the presence (+) or in the absence (-) of *Tfe3* expression vector. All luciferase experiments were performed using Dual-Luciferase Reporter Assay System (Promega, Madison, WI).

10. Small-interfering RNAs

RNA oligonucleotides for *scramble* (5′-UUCUCCGAACGUGUCACGUdTdT-

3′), *Txnip* (forward, 5’-GUCUCUGCUCGAAUUGACAdTdT-3’ (No. 1), 5’-GCAACAUCCUCAAAGUCGAdTdT-3’ (No. 2)) (Genolution, Seoul, Korea) and *Tfe3* (forward, 5′-GCAGGCGAUUCAA CAUUAAdTdT-3′) (GenePharma, Shanghai, China) were synthesized. The siRNA-*Txnip* (20 nmol/l) and siRNA-*Tfe3* (10 nmol/l) were transfected into appropriate experimental sets of primary hepatocytes for 24 h after seeding using Lipofectamine RNA iMAX (Invitrogen, Carlsbad, CA). After 48 h, cells were lysed for RNA isolation and protein extraction.

11. Immunoprecipitation (IP)

Myc or Flag-tagged *Txnip* (2 μg) and HA-tagged *SHP* (2 μg) were co-transfected into HEK293T cells. After 24 h, cells were lysed in cold lysis buffer (50 mmol/l Tris-HCl pH 7.2, 250 mmol/l NaCl, 0.1% NP-40, 2 mmol/l EDTA, 10% (v/v) glycerol) containing appropriate protease inhibitors. The supernatant was precleared with protein A/G PLUS (Santa Cruz, County, CA) and incubated with 2 μl of the indicated antibody, such as anti-Flag (F3165, Sigma-Aldrich, St. Louis, MO), anti-HA (MMS-101R, Covance, Princeton, NJ), or anti-TXNIP (K0205-3, MBL international, Woburn, MA) for 16 h and protein A/G PLUS for additional 4 h at 4°C. Protein pellets were washed 4 times with

lysis buffer, resuspended in sample buffer, and then subjected to SDS-PAGE. For *in vivo* experiments, proteins were extracted from liver using Pro-Prep protein extraction solution (iNtRON, Gyeonggi-do, Korea) and immunoprecipitated with anti-TXNIP.

12. Chromatin immunoprecipitation (ChIP) assay

ChIP experiments on primary hepatocytes were performed as previously described [22]. Briefly, protein extracts were incubated with 4 μg of anti-ChREBP (#NB400-135, NOVUS Biologicals LLC, Littleton, CO) or anti-TFE3 antibodies for 16 h at 4℃. Protein/DNA complexes were precipitated for 1 h at 4℃ using 60 μL of 50% protein A or G agarose/salmon sperm DNA slurry. DNA fragments were purified using a Qiagen PCR purification kit (#28106) and quantified by qPCR. For *in vivo* studies, 50 mg of liver tissue was used for each ChIP assay. The mouse *Txnip* promoter region (-203/-18) with ChoRE was amplified using specific primers (forward, 5'-CGCACCCGAACAACAACCAT -3' and reverse, 5'- GGCTTATATAGCCGCCTGGCTT-3'). As a negative control, the mouse *Txnip* promoter region not included in ChoRE (-907/-773) was amplified using primers (forward, 5'-GCTGCAGTGAGGAACAAGGGAA-3' and reverse, 5'- CTGCTACTGTTCCTCGCCCATT-3').

13. Statistical analysis

Three to five experiments were performed for all *in vitro* studies, using triplicate replicates of each transfection. The data are represented as means ± standard error of the mean (SEM). All data sets were analyzed for statistical significance using a two-tailed unpaired Student's *t* test. All *P* values less than 0.05 were considered significant. Statistical analysis was carried out using SPSS (Ver. 11.5; SPSS Inc. Chicago, IL).

III. RESULTS

1. TXNIP is upregulated in fasting, STZ-diabetic and *db/db* mice liver

To observe the *Txnip* expression in the liver, mice were subjected to fasting and refeeding (Fig. 1A). mRNA level of *Txnip* in the 16 h fasted mice was increased 6-fold compared to ad libitum group *($p<0.05$*) whereas refeeding the mice resulted in a decrease in its mRNA level. A previous study showed that *Txnip* expression is decreased by insulin [12] in the myocytes and adipocytes. However, its expression in the liver was not known yet. As shown in (Fig. 1B and 1C), *Txnip* mRNA expression was decreased in primary cultured hepatocytes in the presence of insulin and refed mice. These data suggest that the expression of *Txnip* could be downregulated by insulin in liver. In fact, hepatic *Txnip* mRNA was upregulated in the type 1 and 2 diabetic model mice, where insulin signaling is impaired (Fig. 1D and 1E) (*$p<0.01$*). And insulin administration resulted in a significant decrease in its mRNA level in these animal models.

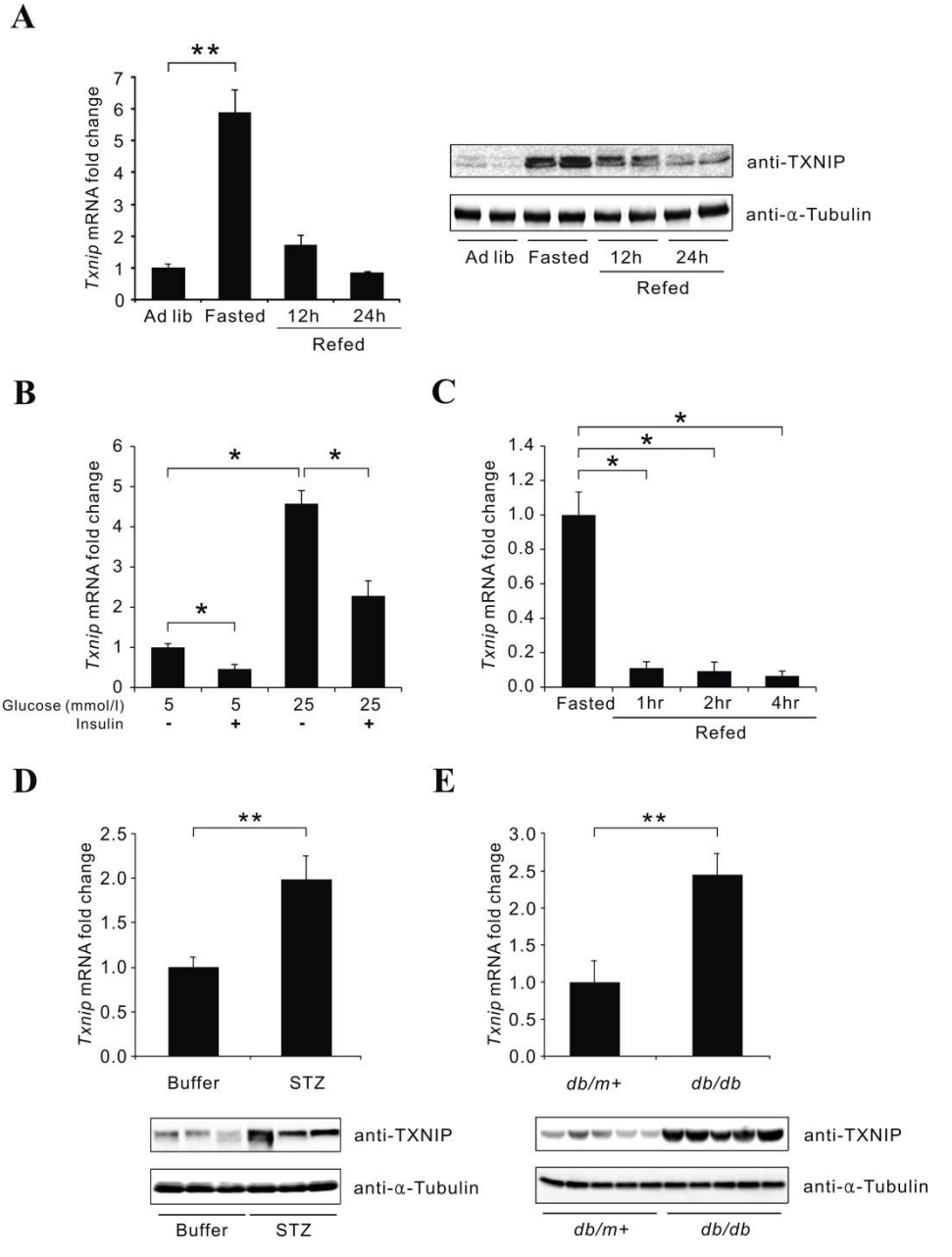
A
**
Txnip mRNA fold change
0
1
2
3
4
5
6
7
Ad lib
Fasted
12h
24h
Refed
anti-TXNIP
anti-α-Tubulin
Ad lib
Fasted
12h
24h
Refed
B
*
*
*
Txnip mRNA fold change
0
1
2
3
4
5
6
Glucose (mmol/l)
Insulin
5
-
5
+
25
-
25
+
C
*
*
*
Txnip mRNA fold change
0.0
0.2
0.4
0.6
0.8
1.0
1.2
1.4
Fasted
1hr
2hr
4hr
Refed
D
**
Txnip mRNA fold change
0.0
0.5
1.0
1.5
2.0
2.5
Buffer
STZ
anti-TXNIP
anti-α-Tubulin
Buffer
STZ
E
**
Txnip mRNA fold change
0.0
0.5
1.0
1.5
2.0
2.5
3.0
db/m+
db/db
anti-TXNIP
anti-α-Tubulin
db/m+
db/db

Figure 1. TXNIP is upregulated in the livers of fasting, STZ-induced diabetic and *db/db* mice

A, Nine-week-old C57BL/6J male mice were fasted 12 h and refed 12 h or 24 h with a chow diet. B, Mouse primary hepatocytes were maintained under the indicated concentrations of glucose (5 and 25 mmol/l) with or without insulin (10 nmol/l). C, Mice fasted 12h and refed with a chow diet at indicated times, respectively. Mice grouped into control (buffer) and STZ-treated mice. STZ-diabetic (D) and *db/db* mice (E) were prepared as described in the text. TXNIP mRNA and protein levels were measured by qPCR and western blot, respectively α-Tubulin was used as an internal control. Data are expressed as the mean ± SEM ($n=8$ per group) (*$p<0.05$, **$p<0.01$). Buffer, buffer control; STZ, streptozotocin.

2. Ad-*Txnip* administration impairs glucose, insulin, and pyruvate tolerance in normal mice

To examine the effects of *Txnip* expression on glucose homeostasis, Ad-*Txnip* was injected via the tail vein into normal mice. Eight days after Ad-*Txnip* injection, intraperitoneal glucose tolerance test (IPGTT) and insulin tolerance test (ITT) were performed. As shown in Fig. 2A and 2B, overexpression of *Txnip* in the liver impairs both glucose and insulin tolerance. An impaired pyruvate tolerance test (PTT) suggested that gluconeogenesis was increased by *Txnip* (Fig. 2C). Furthermore, fasting glucose levels in the Ad-*Txnip* group are significantly higher than those in the Ad-*GFP* group (Fig. 2D). Overexpression of *Txnip* did not change insulin secretion in response to a glucose in vivo (Fig. 2E). Thus, it is speculated that long time term elevation of TXNIP may further impair glucose tolerance.

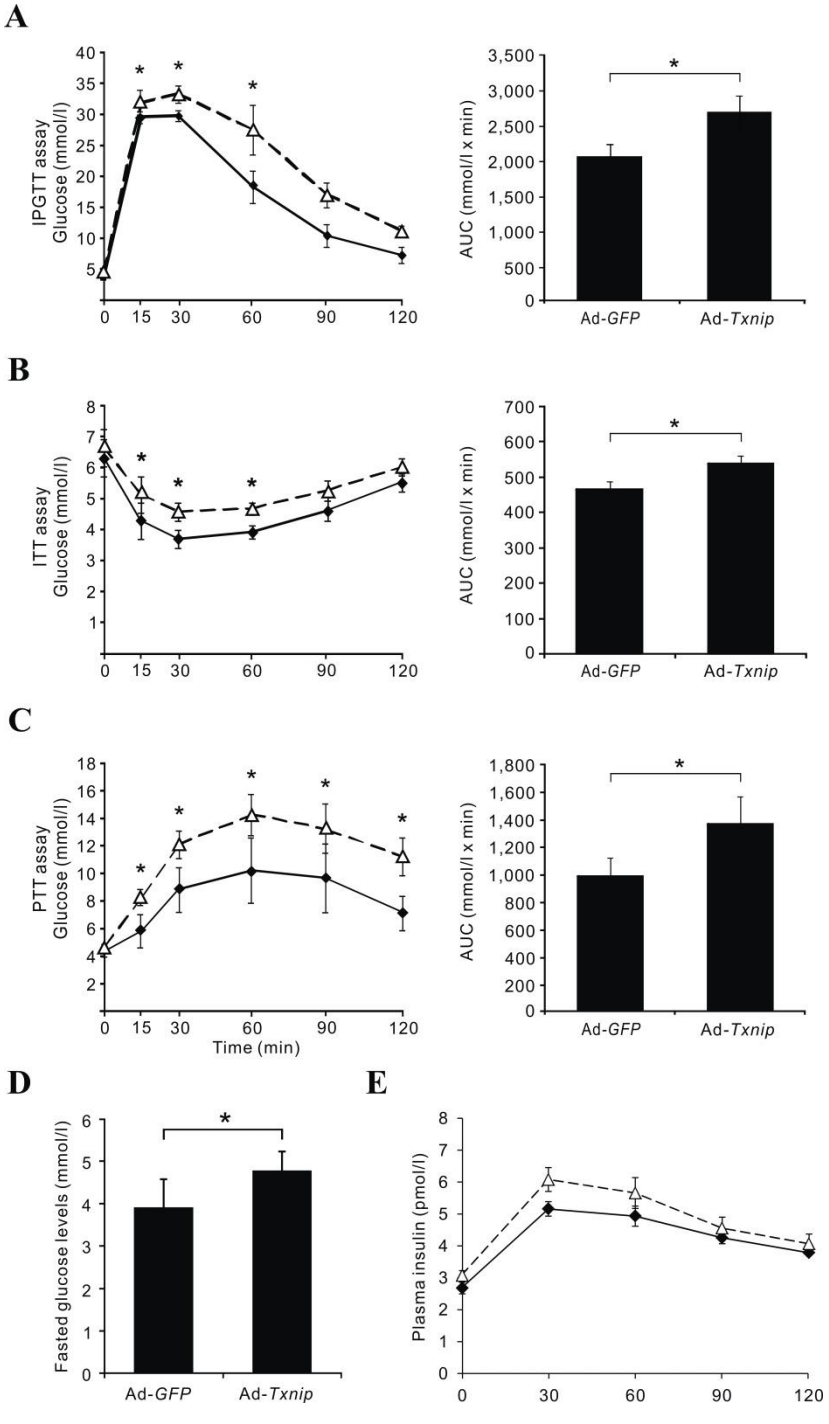
A
IPGTT assay
Glucose (mmol/l)
AUC (mmol/l x min)
Ad-GFP
Ad-Txnip
B
ITT assay
Glucose (mmol/l)
AUC (mmol/l x min)
Ad-GFP
Ad-Txnip
C
PTT assay
Glucose (mmol/l)
Time (min)
AUC (mmol/l x min)
Ad-GFP
Ad-Txnip
D
Fasted glucose levels (mmol/l)
Ad-GFP
Ad-Txnip
E
Plasma insulin (pmol/l)

Figure 2. Ad-*Txnip* administration impairs glucose, insulin, and pyruvate tolerance in normal mice

Eight days after Ad-*Txnip* injection, IPGTT, ITT, and PTT were performed. A, GTT was performed in mice fasted for 16 h. Glucose was injected intraperitoneally. B, For ITT, mice were fasted for 6 h, and insulin was injected intraperitoneally. C, For PTT, mice were fasted for 16 h and injected with sodium pyruvate. Black diamond, Ad-*GFP* injected mice; white triangle, Ad-*Txnip* injected mice. AUC of glucose was calculated during the course of the tests. Blood glucose levels were measured at the indicated time points shown in the Figure. D, The blood glucose levels in the GTT experiment at zero time. E, Plasma insulin levels measured at the indicated time during IPGTT. Data are expressed as the mean ±SEM ($n=8$ per group, $*p<0.05$). GTT, glucose tolerance test; ITT, insulin tolerance test; PTT, pyruvate tolerance test; AUC, area under curve; *GFP*; green fluorescent protein.

3. The effect of Ad-*Txnip* on the expression of genes involved in glucose metabolism in the livers of normal mice

Because TXNIP is responsible for the impaired IPGTT, ITT, and PTT, the expression levels of glycolytic and gluconeogenic genes were quantitated in the liver. As shown (Fig. 3A and 3F, $p<0.01$), *G6pc* expression was significantly increased by *Txnip*; the increase in *Pck1* mRNA expression was not statistically significant (Fig. 3B, $p>0.05$). In contrast, GCK expression was significantly decreased by *Txnip* (Fig. 3D and 3F, $p<0.01$), with a slight increase in *slc2a2* (GLUT2) mRNA levels (Fig. 3C, $p>0.05$). To prove that the impaired glucose and insulin tolerance was not caused by Ad-*Txnip* action in peripheral tissues, the expression of TXNIP in major glucose consumption tissues such as skeletal muscle (Fig. 3G) and adipose tissue (Fig. 3H) was measured. As shown in Fig. 3F, TXNIP overexpression was restricted to the liver. Although the basal glucose level was significantly increased (Fig. 3I, $p<0.05$), the serum insulin level in normal mice was not significantly affected by *Txnip* treatment (Fig. 3J, $p>0.05$). Because upregulation of *Gck* was shown to be accompanied by hepatic lipogenesis [23], the expression of representative genes of lipid metabolism were measured which showed no significant change (Fig. 4). Measurement of glycogen content in the Ad-*Txnip*-treated mice revealed that glycogen content in

this group was not significantly different than controls (Fig. 3K), indicating that G6p is derived from gluconeogenesis.

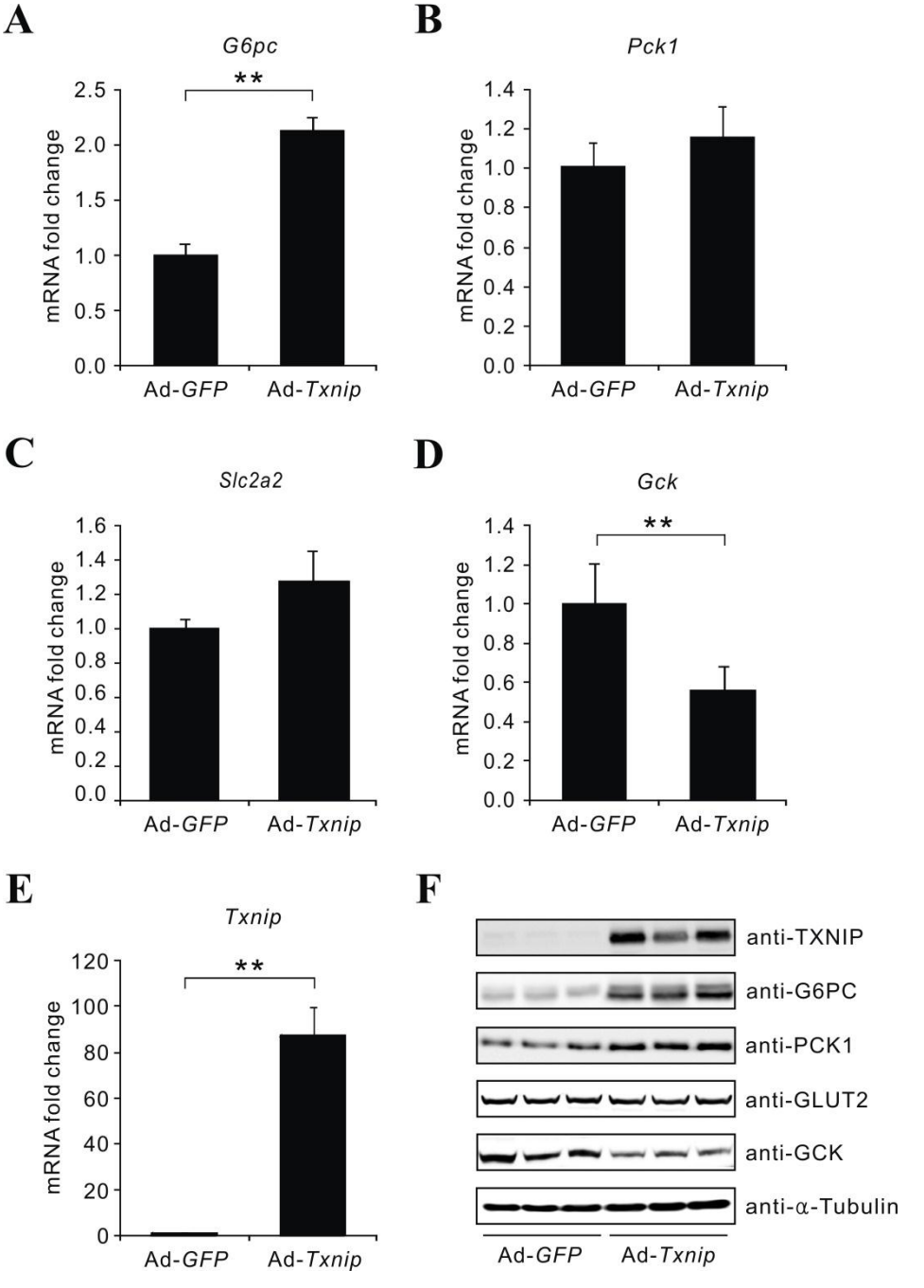
A
G6pc
**
mRNA fold change
2.5
2.0
1.5
1.0
0.5
0.0
Ad-GFP
Ad-Txnip
B
Pck1
mRNA fold change
1.4
1.2
1.0
0.8
0.6
0.4
0.2
0.0
Ad-GFP
Ad-Txnip
C
Slc2a2
mRNA fold change
1.6
1.4
1.2
1.0
0.8
0.6
0.4
0.2
0.0
Ad-GFP
Ad-Txnip
D
Gck
**
mRNA fold change
1.4
1.2
1.0
0.8
0.6
0.4
0.2
0.0
Ad-GFP
Ad-Txnip
E
Txnip
**
mRNA fold change
120
100
80
60
40
20
0
Ad-GFP
Ad-Txnip
F
anti-TXNIP
anti-G6PC
anti-PCK1
anti-GLUT2
anti-GCK
anti-α-Tubulin
Ad-GFP
Ad-Txnip

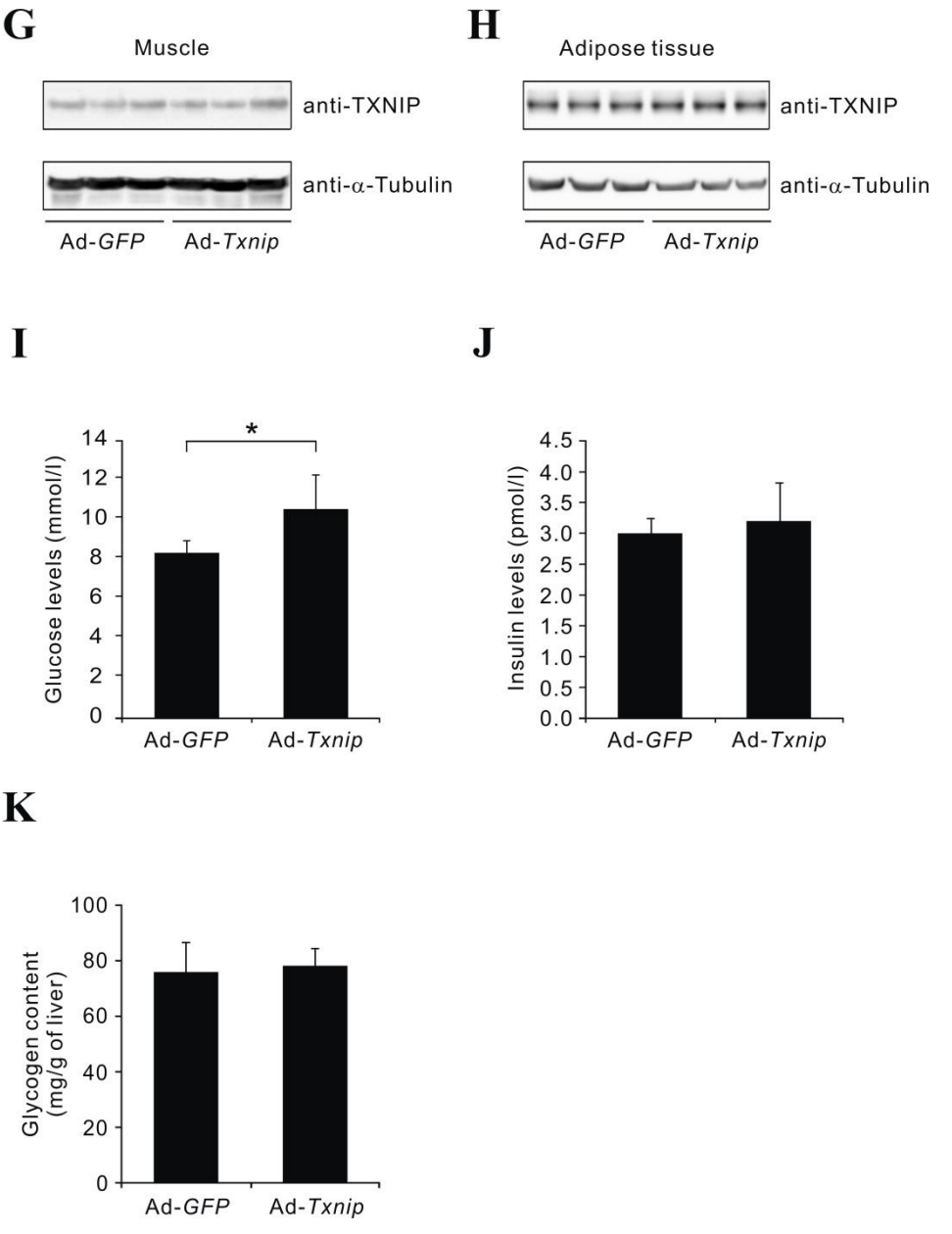

Figure 3. Effect of Ad-*Txnip* on the expression of the genes involved in glucose metabolism in the liver of normal mice

qPCR (A-E) and western blot (F) of genes involved in glucose metabolism in the livers of normal mice injected with Ad-*Txnip*. Each value represents the amount of mRNA relative to that of the Ad-*GFP*-treated group, which was arbitrarily defined as 1. The expression levels of TXNIP on skeletal muscle (G) and adipose tissue (H). The effect of Ad-*Txnip* on the basal serum glucose levels (I), insulin levels (J), and hepatic glycogen content (K). All the values are expressed as the mean ± SEM (*p<0.05, **p<0.01). *G6pc*, glucose-6-phosphatase; *Pck1*, phosphoenol-pyruvate carboxykinase; *Slc2a2*, glucose transporter type 2 isoform; *Gck*, glucokinase.

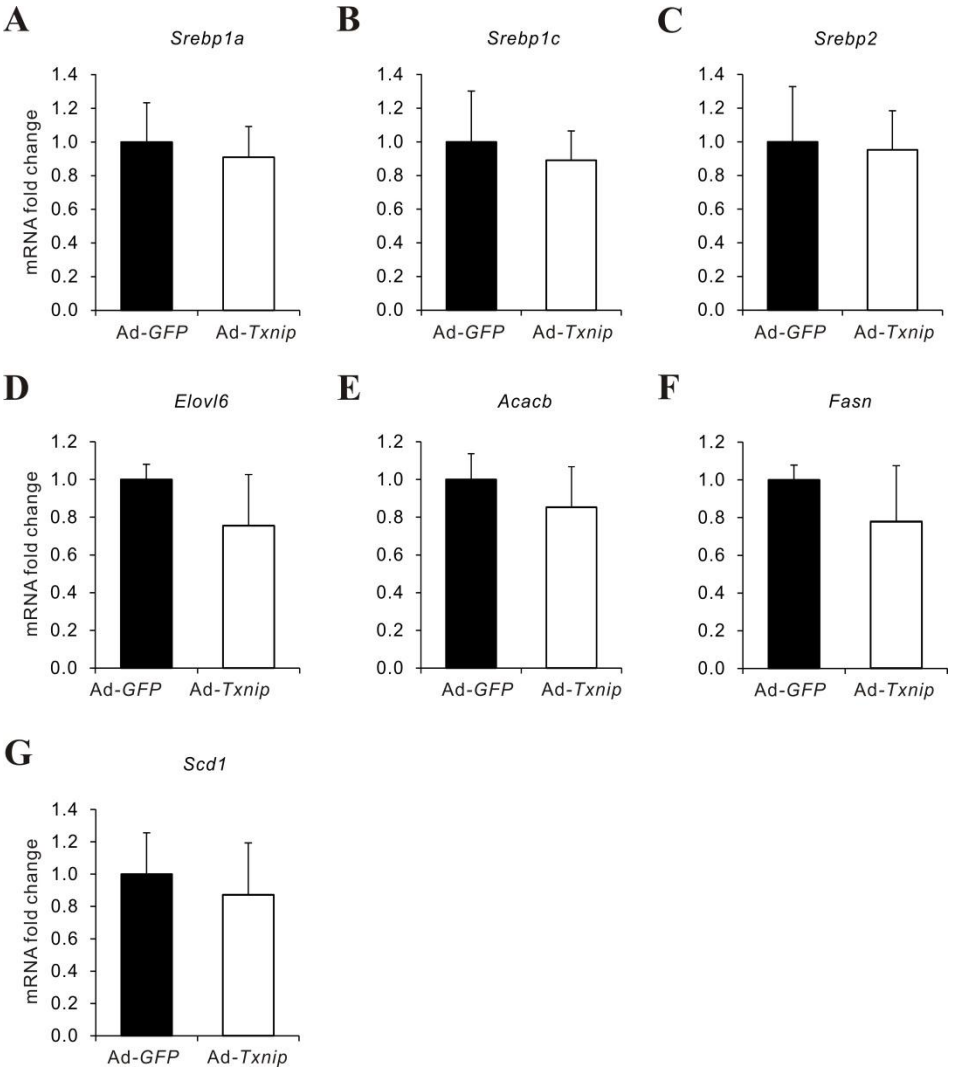

Figure 4. Effect of Ad-*Txnip* on lipogenic gene expression in the liver

A-C. mRNA levels of *Srebp-1a*, *1c* and *2* genes in the livers of normal mice injected with Ad-*Txnip*. D-G. mRNA levels of genes involved in lipid metabolism in the livers of normal mice injected with Ad-*Txnip*. Bars represent the mean ± SEM (n=8). The amount of mRNA in each sample was normalized

to *Rplp0* transcript levels. *Srebp*, Sterol regulatory element-binding protein; *Elovl6*, Elongation of very long chain fatty acids protein 6; *Acacb*, Acetyl-CoA carboxylase beta; *Fasn*, Fatty acid synthase; *Scd1*, Stearoyl-CoA desaturase 1.

4. Transduction of Ad-*Txnip* upregulates *G6pc* expression in primary hepatocytes

To study the direct role of TXNIP on gluconeogenic gene expression in the liver, Ad-*Txnip* was transduced into primary hepatocytes. As shown, G6PC mRNA (Fig. 5A, $p<0.05$) and protein levels (Fig. 5F) were significantly increased by *Txnip*, with marginal increase in PCK1 expression (Fig. 5B and 5F), which correlates well with the *in vivo* experiment (Fig. 3). Similarly, *Txnip* decreased GCK mRNA and protein levels (Fig. 5D and 5F, $p<0.05$) with no significant change in SLC2A2 expression (Fig. 5C and 5F, $p>0.05$). Treatment of hepatocytes with siRNA-*Txnip* (clones si-*Txnip* No. 1 and No. 2) resulted in significantly decreased G6PC expression (Fig. 5G and 5L, $p<0.05$). Although *Pck1* mRNA expression was unchanged (Fig. 5H, $p>0.05$), protein level was slightly decreased (Fig. 5L). In contrast, GCK expression was increased significantly (Fig. 5J and 5L, $p<0.05$) with no change in SCL2A2 expression (Fig. 5I and 5L, $p>0.05$).

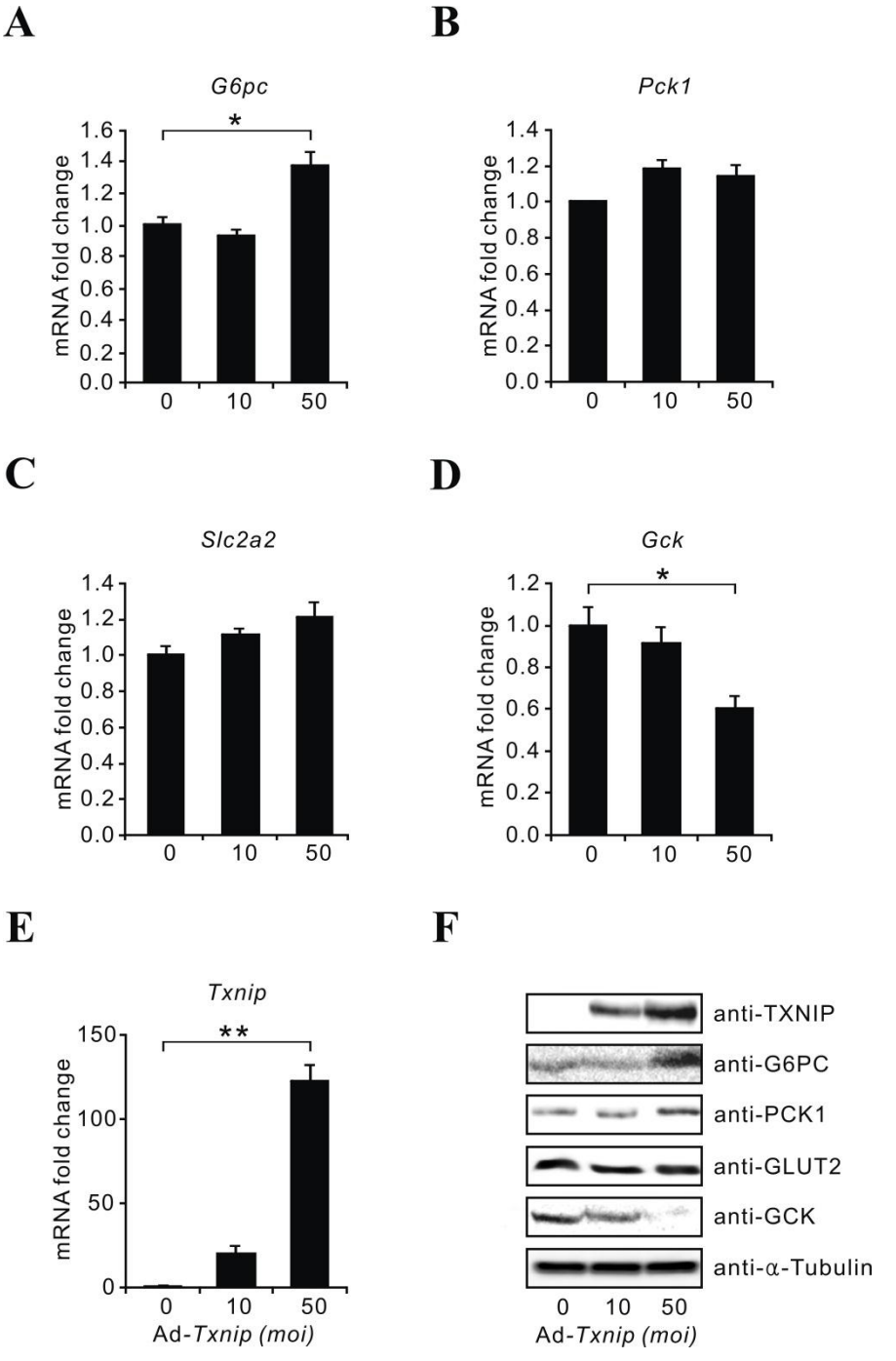
A
G6pc
*
mRNA fold change
1.6
1.4
1.2
1.0
0.8
0.6
0.4
0.2
0.0
0
10
50
B
Pck1
mRNA fold change
1.4
1.2
1.0
0.8
0.6
0.4
0.2
0.0
0
10
50
C
Slc2a2
mRNA fold change
1.4
1.2
1.0
0.8
0.6
0.4
0.2
0.0
0
10
50
D
Gck
*
mRNA fold change
1.2
1.0
0.8
0.6
0.4
0.2
0.0
0
10
50
E
Txnip
**
mRNA fold change
150
100
50
0
0
10
50
Ad-Txnip (moi)
F
anti-TXNIP
anti-G6PC
anti-PCK1
anti-GLUT2
anti-GCK
anti-α-Tubulin
0
10
50
Ad-Txnip (moi)

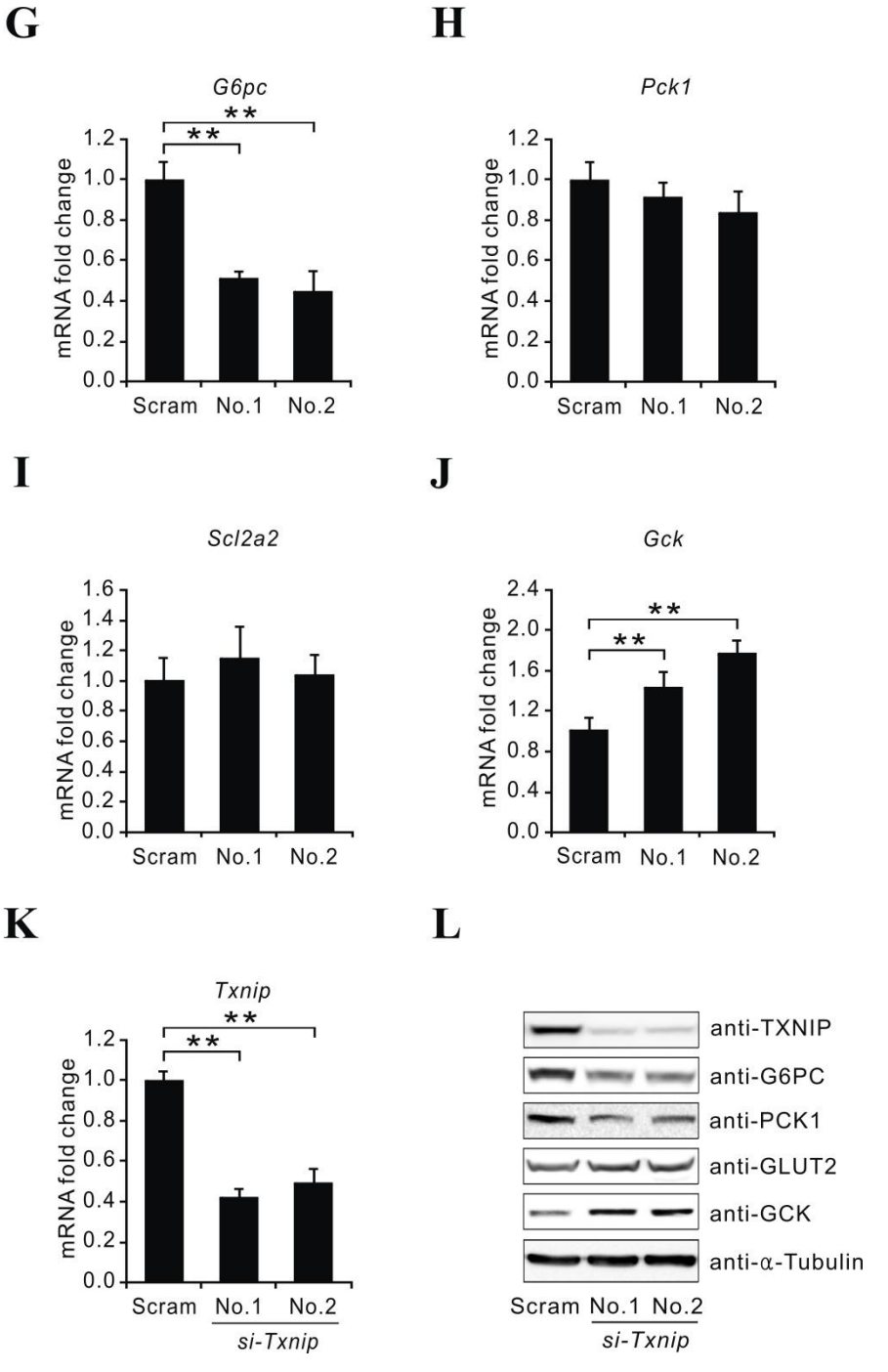
G
G6pc
**
**
mRNA fold change
1.2
1.0
0.8
0.6
0.4
0.2
0.0
Scram
No.1
No.2
H
Pck1
mRNA fold change
1.2
1.0
0.8
0.6
0.4
0.2
0.0
Scram
No.1
No.2
I
Scl2a2
mRNA fold change
1.6
1.4
1.2
1.0
0.8
0.6
0.4
0.2
0.0
Scram
No.1
No.2
J
Gck
**
**
mRNA fold change
2.4
2.0
1.6
1.2
0.8
0.4
0.0
Scram
No.1
No.2
K
Txnip
**
**
mRNA fold change
1.2
1.0
0.8
0.6
0.4
0.2
0.0
Scram
No.1
No.2
si-Txnip
L
anti-TXNIP
anti-G6PC
anti-PCK1
anti-GLUT2
anti-GCK
anti-α-Tubulin
Scram
No.1
No.2
si-Txnip

Figure 5. Transduction of Ad-*Txnip* upregulates *G6pc* expression in primary cultured hepatocytes

Primary cultured hepatocytes were treated with the indicated amounts of Ad-*Txnip*. mRNA levels of *G6pc* (A), *Pck1* (B), *Slc2a2* (C), *Gck* (D), and *Txnip* (E) were measured by qPCR. Each value represents the amount of mRNA relative to that of the Ad-*GFP*-treated group, which was arbitrarily defined as 1. (F) Western blot of G6PC, PCK1, GLUT2, and GCK. The effect of si-*Txnip* on the mRNA (G-K) and protein levels (L) of TXNIP, G6PC, PCK1, GLUT2, and GCK. Scrambled siRNA (*Scram*) or si-*Txnip* (No. 1 and No. 2) was transfected as described in the text. Each value represents the amount of mRNA relative to that of the *Scram* group in the same set of experiments, which was arbitrarily defined as 1. Bars represent the mean ± SEM for three plates per group, performed in triplicate (*p<0.05, **p<0.01). *Scram*: scramble, si-*Txnip*; siRNA-*Txnip*.

5. G6PC expression was increased by TXNIP

To investigate whether *Txnip* expression is correlated with *G6pc* expression in hyperglycemic condition, STZ-diabetic and *db/db* mice models were used. Protein levels of TXNIP and G6PC were increased in the liver of both diabetic models (Fig. 6A and 6B), which were consistent with the mRNA level of *G6pc* in these mice [22, 28].

Because *G6pc* gene expression is regulated by hormones such as glucagon or insulin in vivo [24], effects of glucagon and insulin is observed in terms of TXNIP-*G6pc* relationship. To this end, glucagon was administrated to the Ad-*Txnip*-treated primary cultured hepatocytes (Fig. 6C), which show that *G6pc* expression is increased by 1.5-fold. Knockdown of *Txnip* using siRNA resulted in an inhibition of the glucagon effect (Fig. 6D). When primary cultured hepatocytes were treated with insulin, the expression of *G6pc* was decreased. However, the repressive effect of insulin on *G6pc* expression was rescued by Ad-*Txnip* overexpression (Fig. 6E). Treatment with si-*Txnip* resulted in decreased *G6pc* mRNA levels, which did not further accentuate the insulin effect (Fig. 6F).

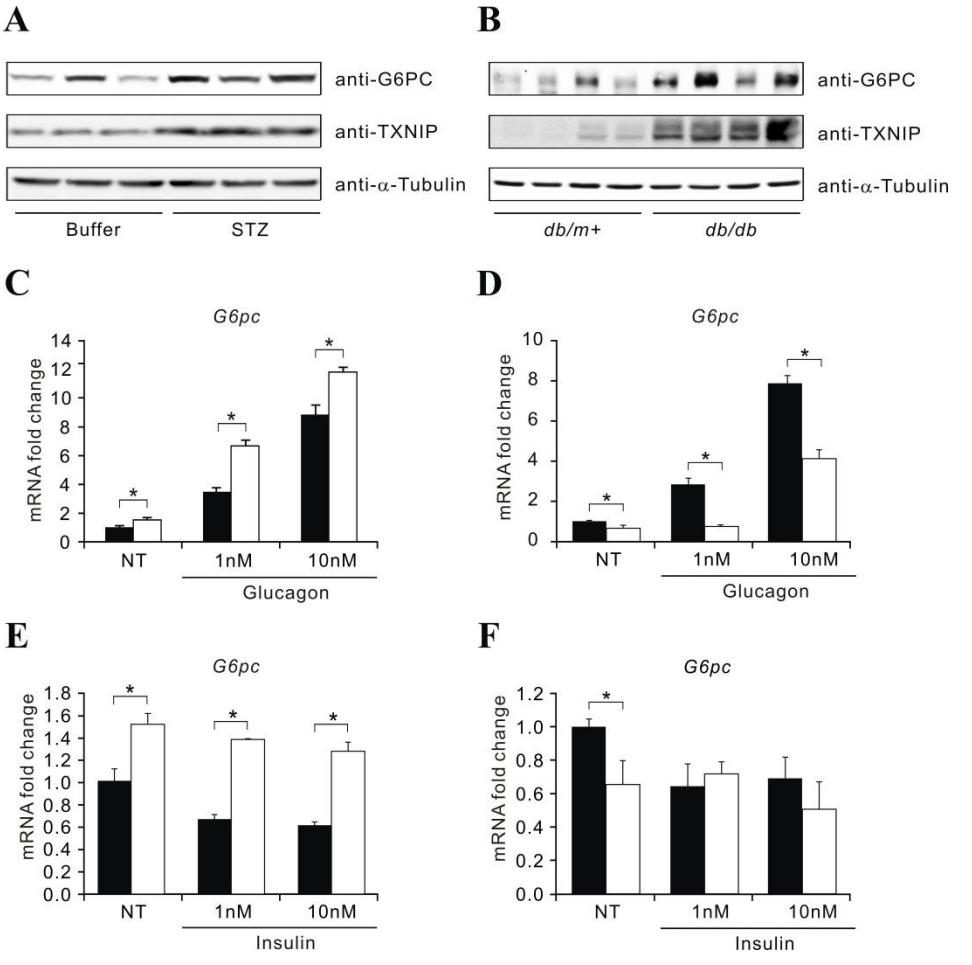

Figure 6. Glucagon potentiates TXNIP-mediated G6PC expression

Western blot of G6PC and TXNIP in the control (buffer), STZ-diabetic and db/db mice. α-Tubulin was used as an internal control. Effect of glucagon on the *G6pc* mRNA level in Ad-*Txnip* (C) and si-*Txnip* (D) treated primary cultured hepatocytes. Effect of insulin on the *G6pc* mRNA level in Ad-*Txnip* (E) and si-

Txnip (F) treated hepatocytes. The hepatocytes were treated with 50 moi of Ad-*Txnip*. After 24 h incubation, culture media were changed with conditioned media containing 1% FBS for 6 h and cells were treated with the indicated amounts of glucagon or insulin for 30 min. Black bar, Ad-*GFP*-treated hepatocyte samples; white bars, Ad-*Txnip*-treated hepatocyte samples. Scrambled siRNA (*Scram*) or si-*Txnip* was transfected as described in the text. After 48 h incubation, culture media were changed as above (*p<0.05). Black bar, Scrambled siRNA-treated hepatocyte samples; white bars, si-*Txnip*-treated hepatocyte samples.

6. SHP negatively modulates transcriptional activities of TXNIP through direct interaction

To better understand how TXNIP upregulates *G6pc*, the effects of TXNIP on the *G6pc* promoter is studied. Activity of this promoter is increased after *Txnip* transfection in a dose dependent manner (Fig. 7A). Co-transfection of *SHP* resulted in a significant decrease in *G6pc* promoter activity both in the negative control and the *Txnip*-transfected group (Fig. 7B, $p<0.05$). In addition, when *Foxo1*, a transcription factor known to increase promoter activity of *G6pc*, was co-transfected with *SHP, Foxo1*-driven promoter activities were decreased as shown in Fig. 7B. Co-transfection of *Foxo1* and *Txnip* increased *G6pc* promoter activity to a greater extent than *Txnip* transfection alone, and transfection of *SHP* to this system resulted in a significant decrease in promoter activity. In addition, *HNFs* mediated *G6pc* promoter activity was also inhibited by SHP (Fig. 7C-E). Immunoprecipitation experiments in 293T cells using myc-*Txnip* or flag-*Txnip* with HA-*SHP* revealed that these two proteins interact with each other (Fig. 7F and 7G). Furthermore, the protein interaction between TXNIP and SHP was increased in the liver of both normal mice which were transduced with Ad-*Txnip* (Fig. 7H) and *db/db* mice (Fig. 7I), suggesting that TXNIP-driven gluconeogenesis is suppressed by SHP.

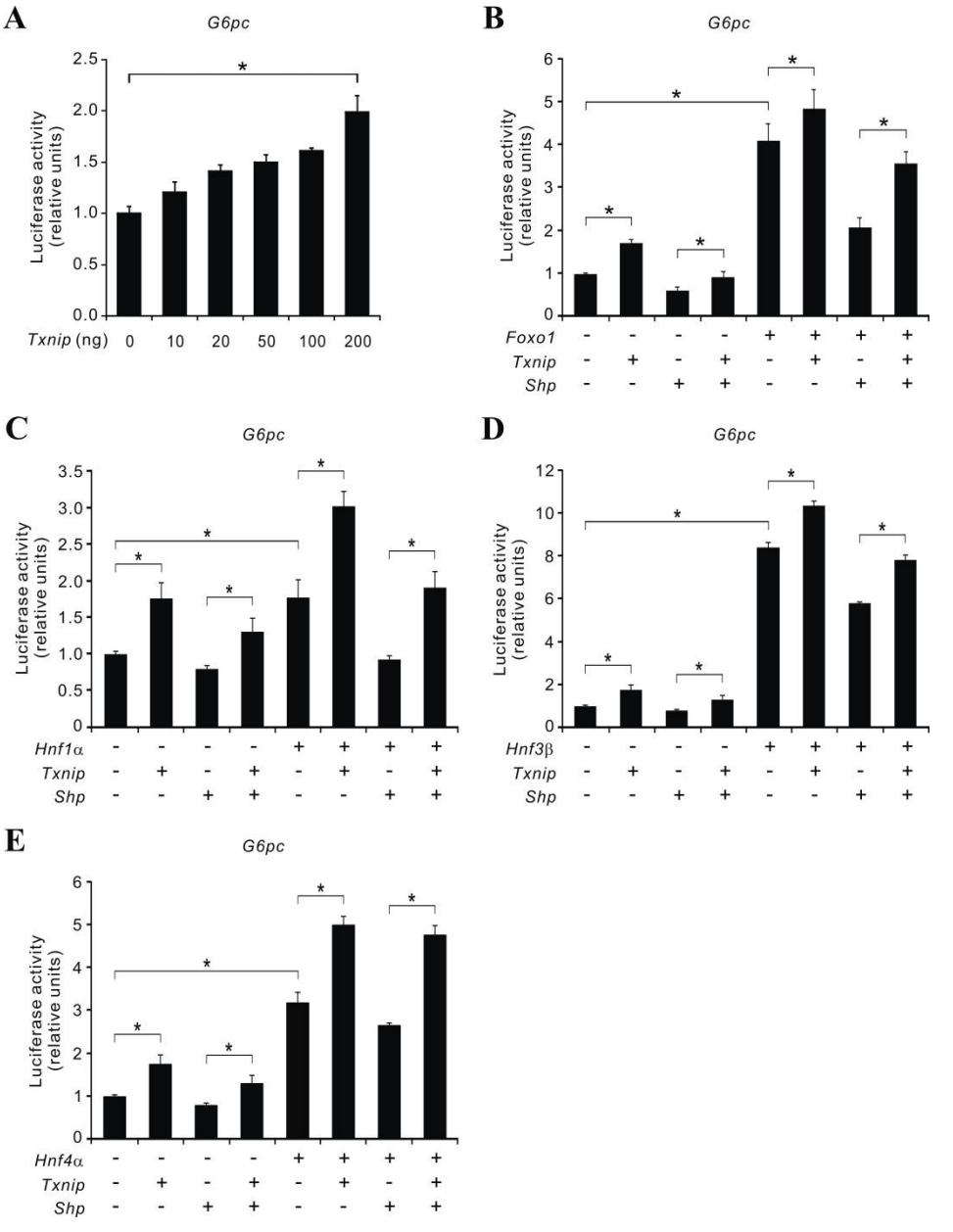
A
G6pc
Luciferase activity (relative units)
Txnip (ng) 0 10 20 50 100 200
B
G6pc
Luciferase activity (relative units)
Foxo1
Txnip
Shp
C
G6pc
Luciferase activity (relative units)
Hnf1α
Txnip
Shp
D
G6pc
Luciferase activity (relative units)
Hnf3β
Txnip
Shp
E
G6pc
Luciferase activity (relative units)
Hnf4α
Txnip
Shp

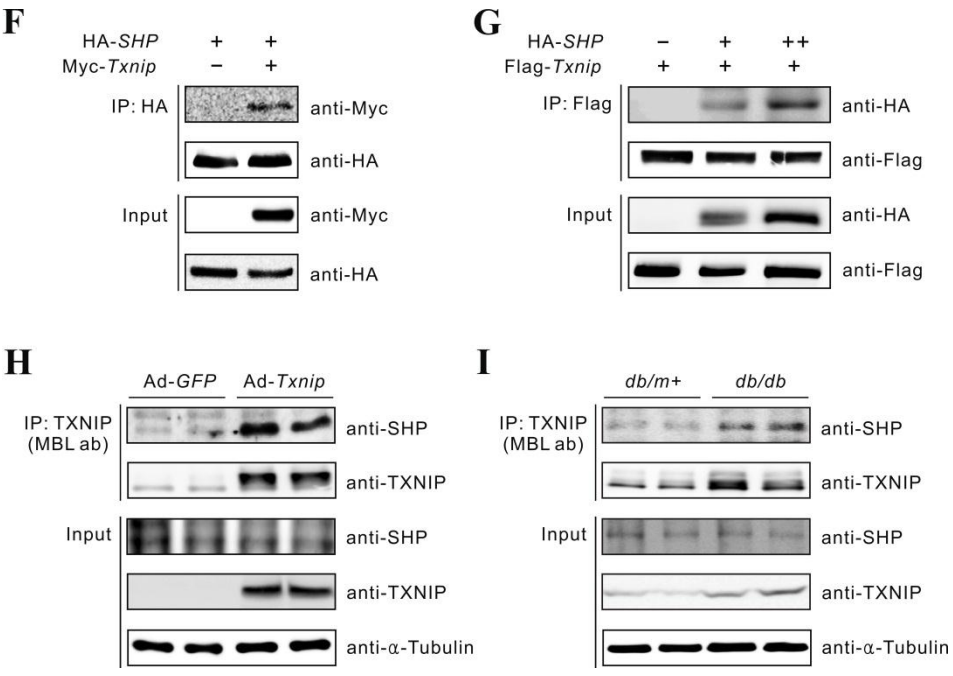

Figure 7. TXNIP negatively modulates transcriptional activity of SHP through direct interaction

A, Effect of *Txnip* on the promoter activity of *G6pc*. HepG2 cells were transfected with *Txnip*, firefly luciferase fusion promoter reporter constructs of *G6pc* (-500/+66 bp) and expression plasmid *Renilla* luciferase. B-E, The effect of *SHP* on the *Txnip*-driven *G6pc* promoter activity in the presence (+) or in the absence (-) of a *Foxo1* (B), *Hnf1α* (C), *Hnf3β* (D) and *Hnf4α* (E) expression vectors. The expression plasmids for *SHP* (200 ng) and *Txnip* (200 ng) were transfected with or without expression vectors (200 ng). Bars represent the

mean ± SEM for three plates per group, performed in triplicate (*p<0.05). F, Identification of interaction between SHP and TXNIP. HA-*SHP* and Myc-*Txnip* were transfected to HEK293T cells. Cell lysates were precipitated with anti-HA antibodies and incubated with anti-Myc antibody. G, Dose response of protein interaction between SHP and TXNIP. Flag-*Txnip* and HA-*SHP* construct (0, 1, and 2 μg) were transfected to HEK293T cells and precipitated with anti-Flag antibodies. Identification of the SHP-TXNIP interaction in the Ad-*Txnip* treated mice or *db/db* mice. H, Ad-*Txnip* (1×10^9 pfu) was injected into tail vein of normal mice. Eight days after infection, the homogenates of liver tissue (50 mg) were precipitated using anti-SHP antibodies. I, Male *db/db* and *db/m*+ mice were sacrificed and used as above. *SHP*, small heterodimer partner.

7. TFE3 downregulates *Txnip* expression in STZ-diabetic and *db/db* mice

Previous study showed that TFE3 upregulates *Gck* in the liver, resulting in the improvement of the GTT and the ITT [22]. Based on this observation, TFE3 could regulate *Txnip* expression in a negative manner. Indeed, Ad-*Tfe3* administration to normal or STZ-diabetic mice resulted in a significant decrease in *Txnip* expression when compared to that of the Ad-*GFP* group (Fig. 8A and 8B). Similarly, *Txnip* expression was significantly decreased by Ad-*Tfe3* either in *db/m*$^{+}$ or *db/db* mice (Fig. 8C and 8D).

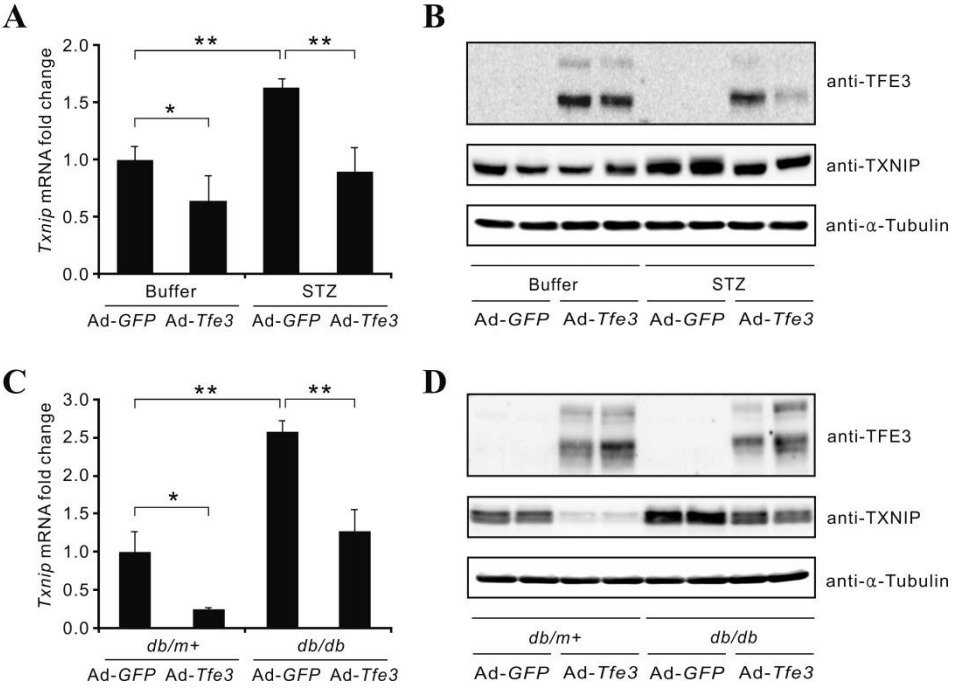

Figure 8. TFE3 downregulates *Txnip* expression in STZ-diabetic and *db/db* mice

The effect of Ad-*Tfe3* on the mRNA and protein level of TXNIP in STZ-diabetic (A and B) and *db/db* mice (C and D). Ad-*GFP* or Ad-*Tfe3* (1×10^7pfu) was injected into the tail vein of STZ-diabetic and *db/db* mice; RNA and protein level were measured, respectively. Bars represent the mean ± SEM (*n*=6, **p*<0.05, ***p*<0.01). TFE3, transcription factor E3.

8. TFE3 and ChREBP regulate the activity of the *Txnip* promoter in a reciprocal manner

To better understand how TFE3 regulates *Txnip* expression, primary hepatocytes were incubated with various concentrations of glucose and with 0, 10, or 50 moi of Ad-*Tfe3*. *Txnip* expression, which increased with glucose concentration, was decreased by Ad-*Tfe3* in a dose dependent manner (Fig. 9A and 9B). Treatment of primary hepatocytes with siRNA-*Tfe3* (si-*Tfe3*) resulted in an increase in *Txnip* mRNA, contrary to the decrease in *Irs2* and *Tfe3* expression (Fig. 9C-F). TFE3 belongs to the Class III basic helix-loop-helix transcription factors, such as the *Srebp* family that binds to E-box [25], and the promoter of *Txnip* contains a non-palindromic E-box (CACGAG). ChREBP, which binds to the E-box of *Txnip* [15], is a key transcription factor activated by glucose in the liver [26]. Thus, it is possible that both of these proteins may bind to the E-box of the *Txnip* promoter. To determine if there is a functional relationship between these proteins on the *Txnip* promoter, a *Txnip* promoter-luciferase construct (-1,119/+279 bp) was transfected with *ChREBP* into HepG2 cells and observed the effect of *Tfe3* on *ChREBP*-driven promoter activity (Fig. 9G). As shown, TFE3 decreased promoter reporter activity in a dose dependent manner. These results suggest that ChREBP and TFE3 act antagonistically on

the E-box. A promoter activity assay using various serial deletion constructs of the *Txnip* promoter revealed that TFE3 suppresses promoter activity of *Txnip* (Fig, 9H). Furthermore, *Tfe3* showed similar inhibitory effect on the ChREBP target genes such as *L-Pk* (Fig. 9I) and *Scd1* (Fig. 9J). To identify TFE3 binding sites, a ChIP assay is performed. As shown, ChREBP binds to the E-box of the promoter in a glucose dependent manner in the absence of TFE3. However, co-transfection of *Tfe3* with *ChREBP* resulted in a decrease of ChREBP binding, even in the presence of high glucose (Fig. 9K). As a negative control, qPCR of the promoter region from -907 to -773 (Fig. 9L), lacking the E-box, revealed that TFE3 binds competitively with ChREBP to the endogenous *Txnip* promoter. Binding of ChREBP to the E-box in STZ-diabetic and *db/db* mice was significantly decreased by the addition of Ad-*Tfe3* (Fig. 9M and N, $p<0.05$).

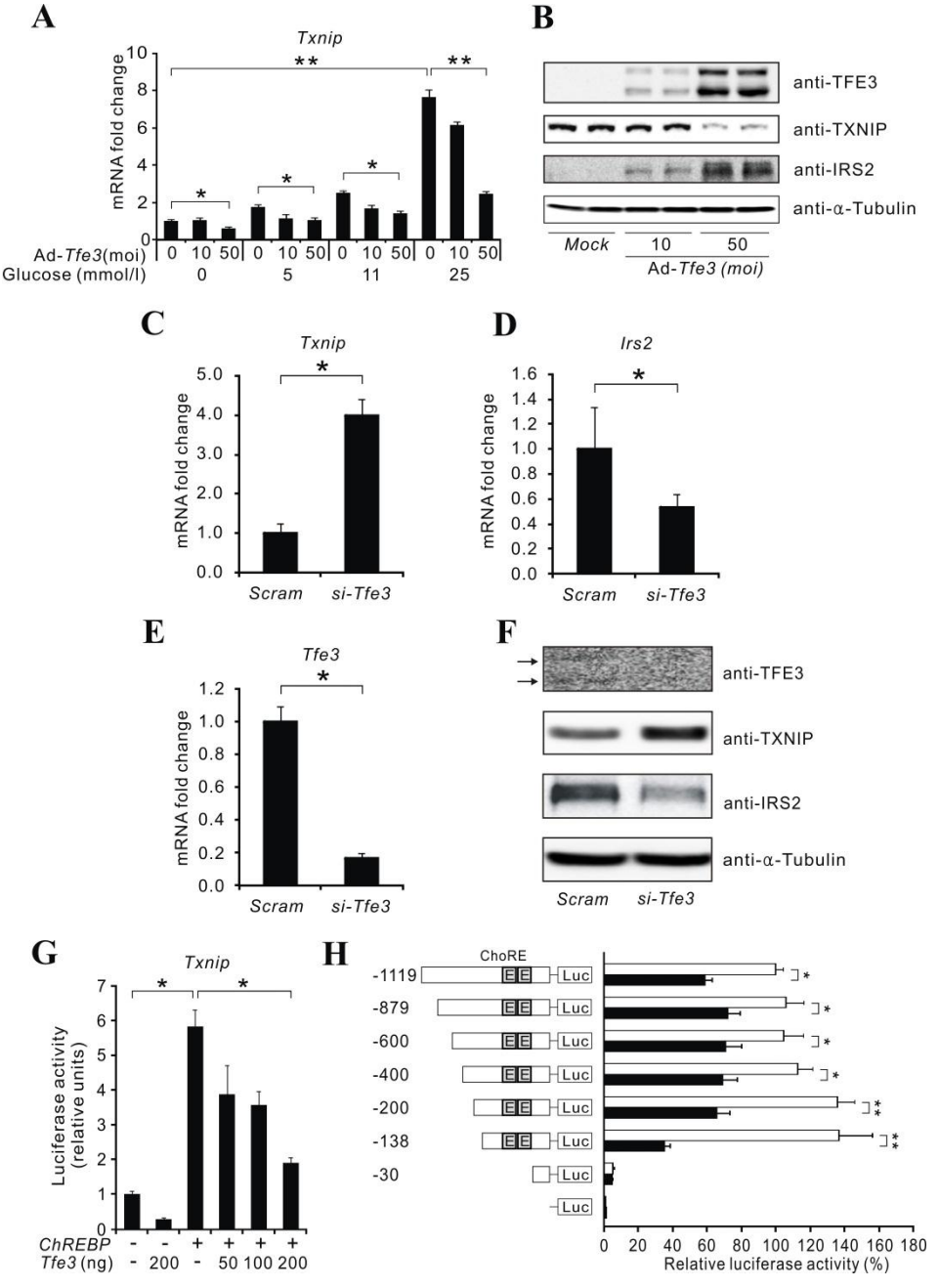
A
Txnip
mRNA fold change
Ad-Tfe3(moi)
Glucose (mmol/l)
B
anti-TFE3
anti-TXNIP
anti-IRS2
anti-α-Tubulin
Mock
Ad-Tfe3 (moi)
C
Txnip
Scram
si-Tfe3
D
Irs2
E
Tfe3
F
G
Luciferase activity (relative units)
ChREBP
Tfe3 (ng)
H
ChoRE
Luc
Relative luciferase activity (%)

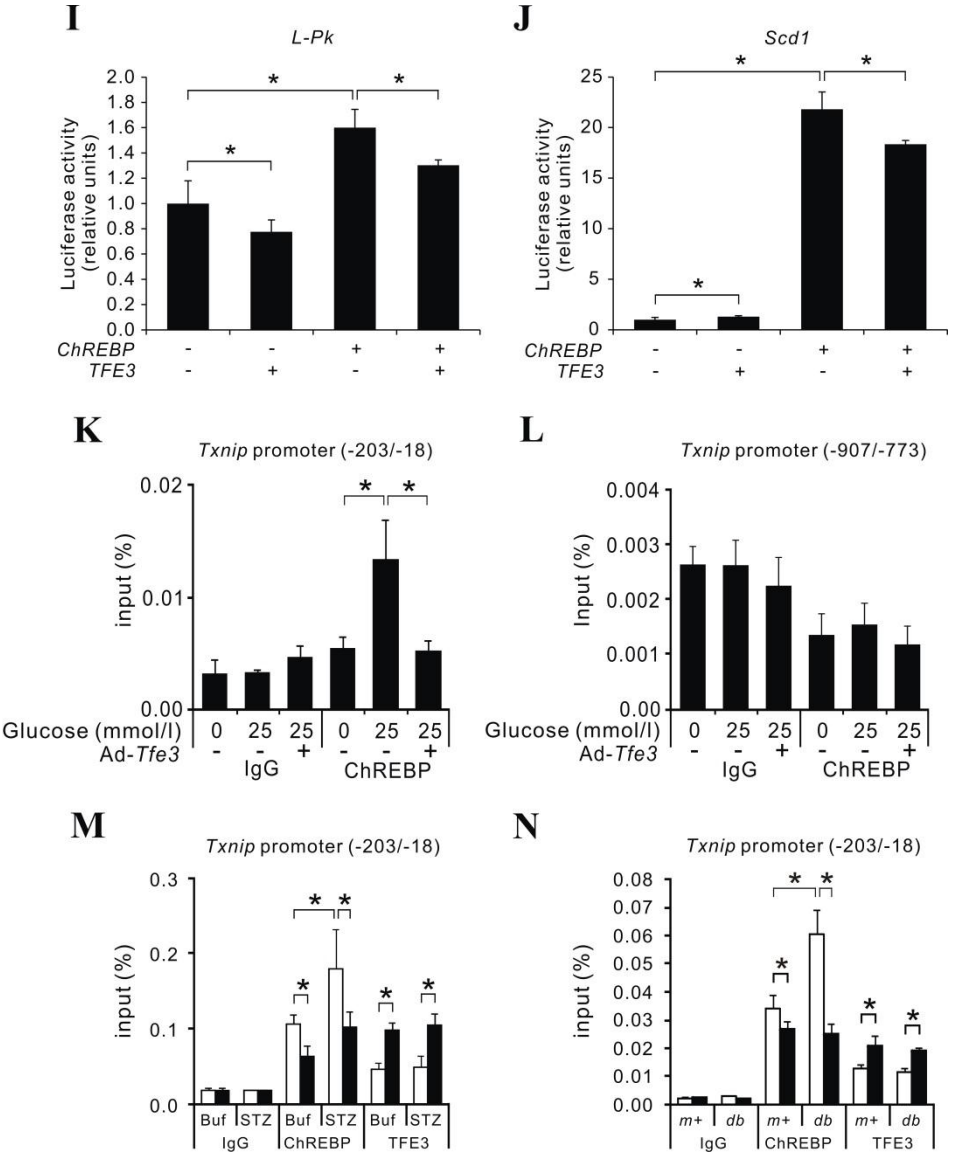

Figure 9. TFE3 and ChREBP regulate the promoter activity of *Txnip* in a reciprocal manner

Mouse primary hepatocytes were maintained under the indicated concentrations of glucose (0. 5, 11, and 25 mmol/l) and Ad-*Tfe3* (0, 10, and 50 moi). After 24 h of Ad-*Tfe3* infection, the mRNA level (A) of *Txnip* (*p<0.05, **p<0.01) and protein level of TFE3, TXNIP, and IRS2 (B) were measured. The effect of si-*Tfe3* on the mRNA (C-E) and protein levels (F) of TXNIP and IRS2. Each value represents the amount of mRNA relative to that of the Ad-*GFP*-treated group, which was arbitrarily defined as 1. Bars represent the mean ± SEM, performed in triplicate. G. The effect of TFE3 on ChREBP-driven *Txnip* promoter activities. HepG2 cells were transfected with the mouse *Txnip* promoter construct from -1119 bp to +279 bp linked to a luciferase reporter gene (200 ng of subcloned *mTxnip*-Luc vectors) and *ChREBP* (200 ng) with the indicated amount of *Tfe3*. H. The effect of TFE3 on ChREBP-driven *Txnip* promoter activities. Various deletion constructs of the *Txnip* promoter and *Tfe3* expression plasmids were co-transfected to HepG2 cells which were cultured under 25 mmol/l glucose. White bars, Empty vector; black bars, *Tfe3* expression vector. Previously reported ChoRE was indicated as a grey box. The effect of *Tfe3* on ChREBP-driven *L-Pk* (I) and *Scd1* (J) promoter activities. HepG2 cells were transfected with firefly luciferase fusion reporter constructs of *L-Pk* (-697/+106 bp) or *Scd1* (-1175/+300 bp) promoter, respectively and expression plasmid

Renilla luciferase in the presence (+) or absence (-) of *ChREBP* or *Tfe3* expression vector as indicated. K and L. A ChIP assay using primary cultured hepatocytes. Hepatocytes were cultured either at 0 or 25 mmol/l glucose in the presence (+) or absence (-) of Ad-*Tfe3*. Cell lysate was precipitated with anti-ChREBP and DNA was amplified using primers shown in Material and Method. Bars represent the mean ± SEM for three plates per group, performed in triplicate. The effect of TFE3 on ChREBP binding to ChoRE in STZ-diabetic (M) and *db/db* mice (N). Normal IgG was used as a negative control. The regions of -203/-18 bp for *Txnip* were amplified. White bar, Ad-*GFP* injected mice liver samples; black bars, Ad-*Tfe3* injected mice liver samples. Bars represent the mean ± SEM (*n=6*). IRS2, insulin receptor substrate 2.

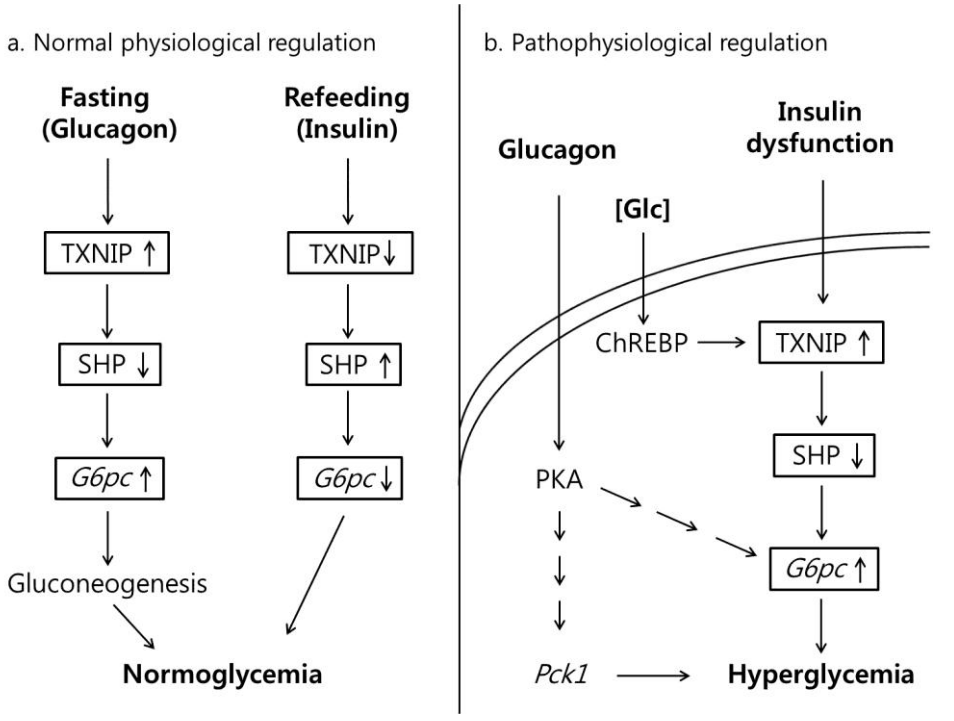

Figure 10. Diagram illustrating the regulation of *G6pc* in the physiological and pathophysiological conditions

A, In the normal states, insulin represses TXNIP expression resulting in downregulation of *G6pc*. B, In the diabetes states, overexpression of *G6pc* occurs through ChREBP-mediated TXNIP upregulation.

IV. DISCUSSION

TXNIP expression is increased in both the hyperglycemic STZ and *db/db* animal models (Fig. 1) and *Txnip* expression is known to be increased in the muscle and adipose tissue of diabetics [12]. A previous study showed that *Txnip*-/- animals exhibit a hypoglycemic phenotype because of increased peripheral glucose utilization and decreased hepatic glucose production [27]. Therefore, it is believed that overexpression of *Txnip* could lead to dysregulation of glucose metabolism and might contribute to hyperglycemia. To determine whether increased expression of *Txnip* in normal liver contributes to the diabetes phenotype, IPGTT, ITT, and PTT were performed (Fig. 2). Overexpression of *Txnip* in the liver by an adenovirus impaired glucose and insulin tolerance due to increased *G6pc* and concomitant decreased *Gck* expression (Fig. 3). In addition, Ad-*Txnip* or siRNA-*Txnip* treatment of primary cultured hepatocytes showed that the level of *G6pc* expression is proportional to that of *Txnip* (Fig. 5A and 5G), whereas the level of *Gck* mRNA is inversely proportional (Fig. 5D and 5J), which was similar to what was observed in an in vivo study. Under physiological conditions, *Txnip* expression is correlated with *G6pc* expression (both are increased in a fasted state and decreased in a refed state [28], and Fig.

1A). In diabetic mice, the expression of TXNIP in the liver is also correlated with that of G6PC [22, 28] (Fig. 6A and 6B).

Because *G6pc* expression is subject to hormonal regulation, it is studied the effects of insulin or glucagon on *Txnip*-mediated *G6pc* expression in primary cultured hepatocytes. Glucagon treatment on Ad-*Txnip*-treated primary hepatocytes increased the expression of *G6pc* 1.5 fold (Fig. 6C). Knockdown of *Txnip* using siRNA inhibited the glucagon effect (Fig. 6D). Although the expression of *Txnip* is not affected by glucagon (data not shown), there may be an additive effect of *Txnip* and glucagon on *G6pc* expression (Fig. 6C and 6D). When primary hepatocytes were treated with insulin, endogenous *Txnip* expression was decreased (Fig. 1B). In a postprandial hyperglycemic state, increased insulin inhibited *Txnip* expression (Fig. 1A and 1C). The repressive effect of insulin on *G6pc* expression was reversed by Ad-*Txnip* overexpression (Fig. 6E). As previously reported, these data suggest that TXNIP could impair insulin signaling [12]. Treatment with si-*Txnip* decreased *G6pc* mRNA levels (Fig. 6F), but did not further increase the insulin effect. It is speculated that there is negative feedback between TXNIP and insulin signaling. However, the molecular mechanism underlying the control of TXNIP expression via insulin signaling in the liver needs to be further studied.

The repression of *Gck* and concomitant induction of *G6pc* in response to high glucose are generally viewed as paradoxical responses [29]. However, the repressive effect of TXNIP on *Gck* expression could be explained by a previous study, which showed that elevated glucose repressed *Gck* gene expression, which facilitates the entry of glucose into the phosphometabolite pool [30]. Furthermore, the induction of *G6pc* by TXNIP might help maintain the homeostasis of phosphorylated intermediates [29] and inhibit glucose uptake [30]. Indeed, several hepatic enzymes are allosterically regulated by Pi, including AMP-deaminase [31]. Patients with mutations that inactivate *G6pc* with Pi depletion have severe hyperuricemia [32]. This result is consistent with the hypothesis that TXNIP-mediated upregulation of *G6pc* expression (Fig. 3A and 5A) contributes to hepatic glucose output and decreases *Gck* levels (Fig. 3D and 5D).

Because TXNIP does not function as a transcription factor, it is searched for transcription factors that could serve as mediators of TXNIP in the regulation of *G6pc* expression. Glucocorticoid receptor (GR) [33], HNF1α [34], HNF3β [35], HNF4α and FOXO1 [36] are positive transcriptional modulators of *G6pc*. SHP is known to suppress gluconeogenesis by forming a complex with these transcription factors [33-36]. *SHP* knockout mice are hyperglycemic in both

the fed and fasted state [37]. Co-transfection with either *Foxo1* or *Hnfs* and a *G6pc* promoter reporter construct increased promoter activity (Fig. 7). The stimulatory effect of these transcription factors was decreased by co-transfection with *SHP*, and the repressive effect of *SHP* was inhibited by *Txnip* in HepG2 cells (Fig. 7). In this study, it is demonstrated that SHP interacts with TXNIP at the protein level both in a cell culture system and in *db/db* mice (Fig. 7F-I) suggesting that TXNIP-SHP complex formation may derepress *G6pc*. In Ad-*Txnip*-transduced primary hepatocytes, SHP protein levels, but not *SHP* mRNA levels, were decreased, suggesting that TXNIP may decrease SHP stability (data not shown). Recent studies have shown that α-arrestin family proteins with a PPxY motif, including TXNIP, bind with an adaptor protein to the E3 ubiquitin ligase ITCH [38-40], resulting in the ubiquitination of both the adaptor protein and TXNIP. Therefore, it is thought that SHP bound to TXNIP could be degraded by ubiquitination. Although TXNIP does not significantly affect *Pck1* mRNA levels (Figs. 3B/5B/5H), it regulates PCK1 protein expression (Figs. 3F/5F/5L). PCK1 is regulated primarily at the transcriptional level [41]; however, recent data suggest that PCK1 degradation is dependent upon acetylation-mediated ubiquitination via recruitment of the UBR5 ubiquitin

ligase [42]. Studies on the ubiquitination of PCK1 in the presence of TXNIP are required to determine if it is involved in the stabilization of PCK1.

In high glucose conditions, *Txnip* expression is increased by ChREBP, which is dephosphorylated and translocated into nucleus [43]. In muscle and adipose tissue, elevated glucose induces the expression of *Txnip* via ChREBP binding to the E-box on the *Txnip* promoter, [12, 15, 44]. Recently, overexpression of the transcription factor *Tfe3* was shown to increase glucose and insulin sensitivity by upregulating the expression of insulin signaling pathway genes, such as *Irs2*, *Akt1*, *Insig1*, *HK2*, and *Gck* by binding to the E-box [21, 22]. Because ChREBP upregulates *Txnip* expression, whereas TFE3 downregulates *Txnip* expression (Fig. 9), it is possible that these two transcription factors will compete for binding to the E-box of the *Txnip* promoter. ChIP assays for ChREBP and TFE3 demonstrated that they bind competitively to the E-box in the *Txnip* promoter (Fig. 9I-L). To confirm the competitive effect of TFE3, it is performed luciferase assays with the promoters of other ChREBP target genes (*L-Pk* and *Scd1*) (Fig. 9G and 9H) and showed that TFE3 has an inhibitory effect on ChREBP activity. In this study, it is overexpressed *Tfe3*, which decreased the binding of ChREBP to the E-box. Because the physiological role of *Tfe3* and its regulation of ChREBP at the levels of transcription and

translation in vivo are not well understood, the relationship between ChREBP and TFE3 in terms of *Txnip* gene regulation is not clear. It is speculated that TFE3 may play an inhibitory role when it binds to the E-Box of the *Txnip* promoter. However, the conditions that regulate the transcriptional activity of *Tfe3* need to be further studied.

Taken together, the expression of *Txnip* is regulated by ChREBP and TFE3 to the control of hepatic gluconeogenic gene expression. *Txnip* overexpression relieves SHP-dependent *G6pc* repression. Consequently, hepatic gluconeogenesis is increased by *Txnip* overexpression leading to reducing systemic glucose tolerance and insulin sensitivity. The physiological and pathophysiological regulation of gluconeogenic gene expression by TXNIP is illustrated in Fig. 10.

V. CONCLUSION

TXNIP is upregulated in fasting, STZ-diabetic and *db/db* mice liver and administration of Ad-*Txnip* into normal mice impairs glucose, insulin sensitivity and pyruvate tolerance. When TXNIP expression was increased by hyperglycemia in pathogenic condition such as diabetes mellitus, TXNIP increased *G6pc* expression by forming a complex with SHP, which is known to be a negative modulator of gluconeogenesis. *Txnip* expression in mouse models of diabetes was decreased by Ad-*Tfe3* administration, suggesting that TFE3 may play a antagonistic role by competitive binding of the promoter regions (E-box) of ChREBP target genes.

REFERENCES

1. Hotamisligil GS. Inflammation and metabolic disorders. Nature 2006;444 (7121):860-7.
2. Herman MA, Kahn BB. Glucose transport and sensing in the maintenance of glucose homeostasis and metabolic harmony. J Clin Invest. 2006;116 (7):1767-75.
3. Pryor HJ, Smyth JE, Quinlan PT, Halestrap AP. Evidence that the flux control coefficient of the respiratory chain is high during gluconeogenesis from lactate in hepatocytes from starved rats. Implications for the hormonal control of gluconeogenesis and action of hypoglycaemic agents. Biochem J 1987;247(2):449-57.
4. Hausler N, Browning J, Merritt M, Storey C, Milde A, Jeffrey FM, et al. Effects of insulin and cytosolic redox state on glucose production pathways in the isolated perfused mouse liver measured by integrated 2H and 13C NMR. Biochem J 2006;394(Pt 2):465-73.
5. Kahn SE, Hull RL, Utzschneider KM. Mechanisms linking obesity to insulin resistance and type 2 diabetes. Nature 2006;444(7121):840-6.
6. Meuillet EJ, Mahadevan D, Berggren M, Coon A, Powis G. Thioredoxin-1 binds to the C2 domain of PTEN inhibiting PTEN's lipid phosphatase activity and membrane binding: a mechanism for the functional loss of PTEN's tumor suppressor activity. Arch Biochem Biophys 2004;429 (2):123-33.

7. Das KC, Das CK. Thioredoxin, a singlet oxygen quencher and hydroxyl radical scavenger: redox independent functions. Biochem Biophys Res Commun 2000;277(2):443-7.
8. Spindel ON, World C, Berk BC. Thioredoxin interacting protein: redox dependent and independent regulatory mechanisms. Antioxid Redox Signal 2012;16(6):587-96.
9. Stienstra R, Tack CJ, Kanneganti TD, Joosten LA, Netea MG. The inflammasome puts obesity in the danger zone. Cell Metab 2012;15(1):10-8.
10. Donath MY, Storling J, Maedler K, Mandrup-Poulsen T. Inflammatory mediators and islet beta-cell failure: a link between type 1 and type 2 diabetes. J Mol Med (Berl) 2003;81(8):455-70.
11. Dinarello CA, Donath MY, Mandrup-Poulsen T. Role of IL-1beta in type 2 diabetes. Curr Opin Endocrinol Diabetes Obes 2010;17(4):314-21.
12. Parikh H, Carlsson E, Chutkow WA, Johansson LE, Storgaard H, Poulsen P, et al. TXNIP regulates peripheral glucose metabolism in humans. PLoS Med 2007;4(5):e158.
13. Papadia S, Soriano FX, Leveille F, Martel MA, Dakin KA, Hansen HH, et al. Synaptic NMDA receptor activity boosts intrinsic antioxidant defenses. Nat Neurosci 2008;11(4):476-87.
14. Schulze PC, Liu H, Choe E, Yoshioka J, Shalev A, Bloch KD, et al. Nitric oxide-dependent suppression of thioredoxin-interacting protein expression enhances thioredoxin activity. Arterioscler Thromb Vasc Biol 2006;26(12):2666-72.
15. Cha-Molstad H, Saxena G, Chen J, Shalev A. Glucose-stimulated expression

of Txnip is mediated by carbohydrate response element-binding protein, p300, and histone H4 acetylation in pancreatic beta cells. J Biol Chem 2009;284(25):16898-905.

16. Reich E, Tamary A, Sionov RV, Melloul D. Involvement of thioredoxin-interacting protein (TXNIP) in glucocorticoid-mediated beta cell death. Diabetologia 2012;55(4):1048-57.
17. Chen KS, DeLuca HF. Isolation and characterization of a novel cDNA from HL-60 cells treated with 1,25-dihydroxyvitamin D-3. Biochim Biophys Acta 1994;1219(1):26-32.
18. Qi W, Chen X, Holian J, Tan CY, Kelly DJ, Pollock CA. Transcription factors Kruppel-like factor 6 and peroxisome proliferator-activated receptor-{gamma} mediate high glucose-induced thioredoxin-interacting protein. Am J Pathol 2009;175(5):1858-67.
19. Zhou R, Tardivel A, Thorens B, Choi I, Tschopp J. Thioredoxin-interacting protein links oxidative stress to inflammasome activation. Nat Immunol 2010;11(2):136-40.
20. Billiet L, Furman C, Larigauderie G, Copin C, Page S, Fruchart JC, et al. Enhanced VDUP-1 gene expression by PPARgamma agonist induces apoptosis in human macrophage. J Cell Physiol 2008;214(1):183-91.
21. Nakagawa Y, Shimano H, Yoshikawa T, Ide T, Tamura M, Furusawa M, et al. TFE3 transcriptionally activates hepatic IRS-2, participates in insulin signaling and ameliorates diabetes. Nat Med 2006;12(1):107-13.
22. Kim MY, Jo SH, Park JM, Kim TH, Im SS, Ahn YH. Adenovirus-mediated overexpression of Tcfe3 ameliorates hyperglycaemia in a mouse model of

diabetes by upregulating glucokinase in the liver. Diabetologia 2013;56(3):635-43.

23. Peter A, Stefan N, Cegan A, Walenta M, Wagner S, Konigsrainer A, et al. Hepatic glucokinase expression is associated with lipogenesis and fatty liver in humans. J Clin Endocrinol Metab 2011;96(7):E1126-30.
24. Argaud D, Zhang Q, Pan W, Maitra S, Pilkis SJ, Lange AJ. Regulation of rat liver glucose-6-phosphatase gene expression in different nutritional and hormonal states: gene structure and 5'-flanking sequence. Diabetes. 1996 ;45(11):1563-71.
25. Massari ME, Murre C. Helix-loop-helix proteins: regulators of transcription in eucaryotic organisms. Mol Cell Biol 2000;20(2):429-40.
26. Yamashita H, Takenoshita M, Sakurai M, Bruick RK, Henzel WJ, Shillinglaw W, et al. A glucose-responsive transcription factor that regulates carbohydrate metabolism in the liver. Proc Natl Acad Sci U S A 2001;98(16):9116-21.
27. Chutkow WA, Patwari P, Yoshioka J, Lee RT. Thioredoxin-interacting protein (Txnip) is a critical regulator of hepatic glucose production. J Biol Chem 2008;283(4):2397-406.
28. Im SS, Kim MY, Kwon SK, Kim TH, Bae JS, Kim H, et al. Peroxisome proliferator-activated receptor {alpha} is responsible for the up-regulation of hepatic glucose-6-phosphatase gene expression in fasting and db/db Mice. J Biol Chem 2011;286(2):1157-64.
29. Agius L. High-carbohydrate diets induce hepatic insulin resistance to protect the liver from substrate overload. Biochem Pharmacol 2013;85(3):306-12.

30. Arden C, Petrie JL, Tudhope SJ, Al-Oanzi Z, Claydon AJ, Beynon RJ, et al. Elevated glucose represses liver glucokinase and induces its regulatory protein to safeguard hepatic phosphate homeostasis. Diabetes 2011;60(12):3110-20.
31. Mayes PA. Intermediary metabolism of fructose. Am J Clin Nutr 1993;58(5 Suppl):754S-65S.
32. Chou JY, Mansfield BC. Mutations in the glucose-6-phosphatase-alpha (G6PC) gene that cause type Ia glycogen storage disease. Hum Mutat 2008;29(7):921-30.
33. Borgius LJ, Steffensen KR, Gustafsson JA, Treuter E. Glucocorticoid signaling is perturbed by the atypical orphan receptor and corepressor SHP. J Biol Chem 2002;277(51):49761-6.
34. Jung D, Kullak-Ublick GA. Hepatocyte nuclear factor 1 alpha: a key mediator of the effect of bile acids on gene expression. Hepatology 2003;37(3):622-31.
35. Kim JY, Kim HJ, Kim KT, Park YY, Seong HA, Park KC, et al. Orphan nuclear receptor small heterodimer partner represses hepatocyte nuclear factor 3/Foxa transactivation via inhibition of its DNA binding. Mol Endocrinol 2004;18(12):2880-94.
36. Yamagata K, Daitoku H, Shimamoto Y, Matsuzaki H, Hirota K, Ishida J Y, et al. Bile acids regulate gluconeogenic gene expression via small heterodimer partner-mediated repression of hepatocyte nuclear factor 4 and Foxo1. J Biol Chem 2004;279(22):23158-65.

37. Ma K, Saha PK, Chan L, Moore DD. Farnesoid X receptor is essential for normal glucose homeostasis. J Clin Invest 2006;116(4):1102-9.
38. Lin CH, MacGurn JA, Chu T, Stefan CJ, Emr SD. Arrestin-related ubiquitin-ligase adaptors regulate endocytosis and protein turnover at the cell surface. Cell 2008;135(4):714-25.
39. Rauch S, Martin-Serrano J. Multiple interactions between the ESCRT machinery and arrestin-related proteins: implications for PPXY-dependent budding. J Virol 2011;85(7):3546-56.
40. Zhang P, Wang C, Gao K, Wang D, Mao J, An J, et al. The ubiquitin ligase itch regulates apoptosis by targeting thioredoxin-interacting protein for ubiquitin-dependent degradation. J Biol Chem 2010;285(12):8869-79.
41. Hanson RW, Reshef L. Regulation of phosphoenolpyruvate carboxykinase (GTP) gene expression. Annu Rev Biochem 1997;66:581-611.
42. Jiang W, Wang S, Xiao M, Lin Y, Zhou L, Lei Q, et al. Acetylation regulates gluconeogenesis by promoting PEPCK1 degradation via recruiting the UBR5 ubiquitin ligase. Mol Cell 2011;43(1):33-44.
43. Poupeau A, Postic C. Cross-regulation of hepatic glucose metabolism via ChREBP and nuclear receptors. Biochim Biophys Acta 2011;1812(8):995-1006.
44. Stoltzman CA, Peterson CW, Breen KT, Muoio DM, Billin AN, Ayer DE. Glucose sensing by MondoA:Mlx complexes: a role for hexokinases and direct regulation of thioredoxin-interacting protein expression. Proc Natl Acad Sci U S A 2008;105(19):6912-7.

Abstract (in Korean)

간 조직의 포도당항상성 유지에서 TXNIP의 역할

<지도교수 안 용 호>

연세대학교 의과대학 의과학과

조 성 호

Thioredoxin interacting protein (TXNIP)는 활성산소종의 발생, 세포사멸, 염증반응 그리고 세포의 포도당 대사과정 등에서 다양한 역할을 한다. TXNIP는 고혈당 상태에서 발현이 증가되고 다양한 조직에서 포도당 흡수를 저해하여 체내 포도당 항상성의 불균형을 일으킨다. 비록 TXNIP가 포도당 대사과정과 관련된 대사성 질환인

비만과 제 1, 2형 당뇨병과 관련이 있다고 보고되어 있지만 간장에서 TXNIP의 역할은 자세히 보고되지 않았다. 본 연구에서는 간장에서 대사성 질환과 관련된 TXNIP의 역할을 밝히기 위하여 생쥐의 간에 TXNIP가 결합된 아데노바이러스 (Ad-*Txnip*)를 처리하여 복강 내 당부하 검사 (IPGTT), 인슐린 저항성 검사 (ITT) 그리고 피루브산염 저항성 검사 (PTT)를 시행하였고 그 결과 저항성이 약화되는 것을 보였다. Ad-*Txnip*의 처리 후, 생쥐의 간장조직과 일차 간세포 배양에서 실시간 중합효소연쇄반응 (qPCR)과 웨스턴블롯 분석을 이용하여 글루코오스-6-포스파타아제 (*G6pc*)의 발현 증가와 클루코키나아제 (*Gck*)의 발현 감소를 확인하였다. 간장 조직에서 증가된 TXNIP 발현에 따른 *G6pc* 발현 증가를 연구하기 위하여 포도당신생합성 과정에서 저해적인 역할을 하는 small heterodimer partner (SHP)와 TXNIP의 상호작용을 확인하고 이에 따라 *G6pc*의 발현이 조절되는 것을 확인하였다. 그리고 *Txnip* 유전자 발현조절을 연구하기 위하여 *Txnip* promoter를 이용한 luciferase assay와 염색질 면역침전반응 (ChIP)을 수행하여 *Txnip* 발현을 조절하는 carbohydrate response element binding protein (ChREBP)와 transcription factor E3 (TFE3)의 연관성을 확인하였다. 뿐만 아니라 당뇨병 질환 생쥐 모델에 TFE3가 결합된 아데노바이러스 (Ad-*Tfe3*)를 처리하여 *Txnip* 발현이 감소하는 것을

확인하고 이는 TFE3가 *Txnip* promoter의 E-box에서 ChREBP와 경쟁적인 관계를 통해 *Txnip*의 발현을 저해하는 역할을 한다고 추정된다. 이런 발견은 TXNIP가 SHP와 상호작용을 통하여 *G6pc* 발현이 증가하여 포도당 및 인슐린 저항성을 약화시키며 이를 조절하는 것은 당뇨병에 의한 고혈당 상태를 개선하는데 도움이 된다고 설명할 수 있다.

핵심되는 말: TXNIP, SHP, ChREBP, TFE3, G6PC, GCK, 포도당신생합성, 전사적 조절